AD-A054 226 OPTICAL COATING LAB INC CITY OF INDUSTRY CA PHOTOELE--ETC F/G 10/2
HIGH OUTPUT SOLAR CELL WITH MULTILAYER AR COATING.(U)
NOV 77 P ILES F33615-76-C-2166

UNCLASSIFIED AFAPL-TR-77-71 NL

| OF |
AD
A054226

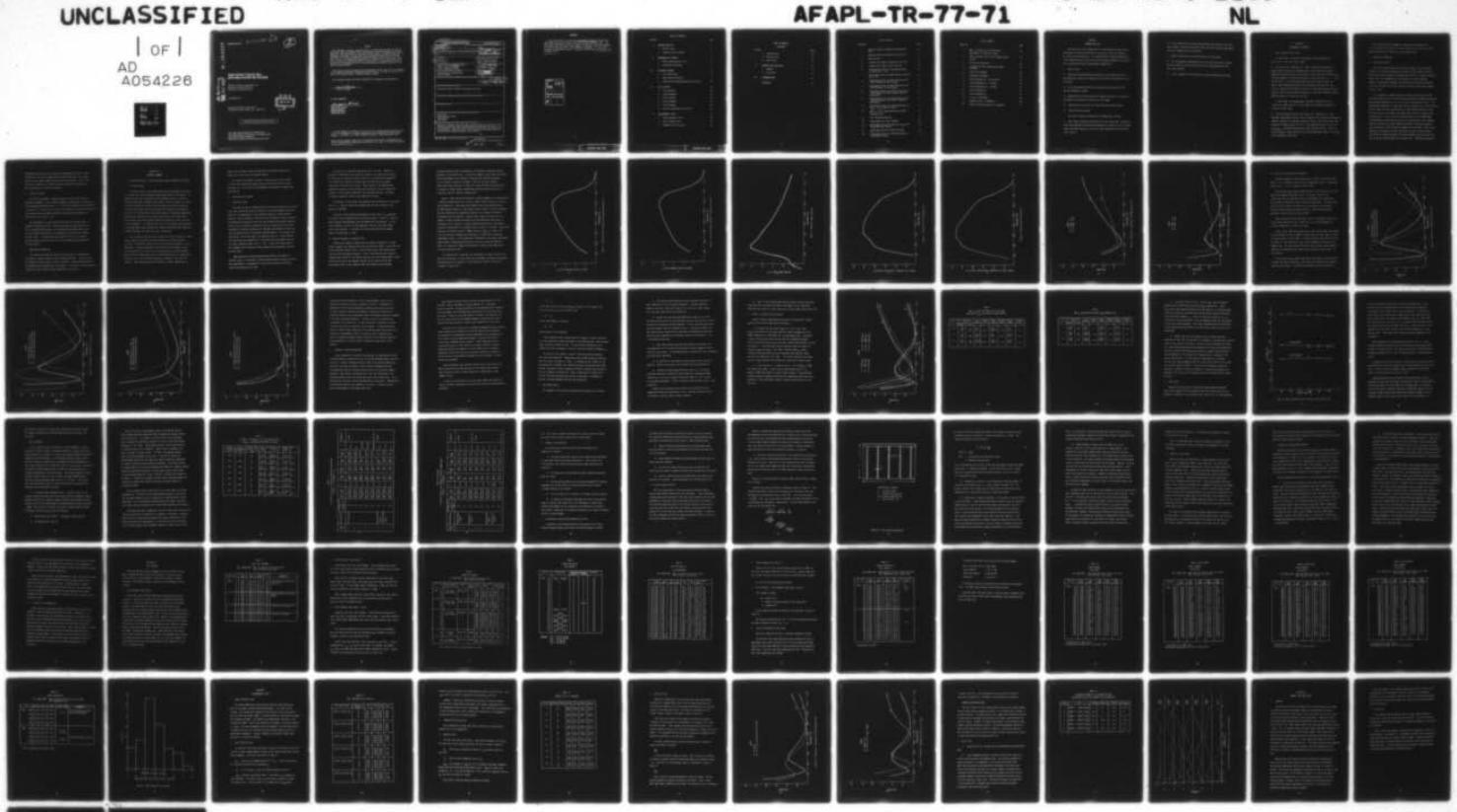

END
DATE
FILMED
6-78
DDC

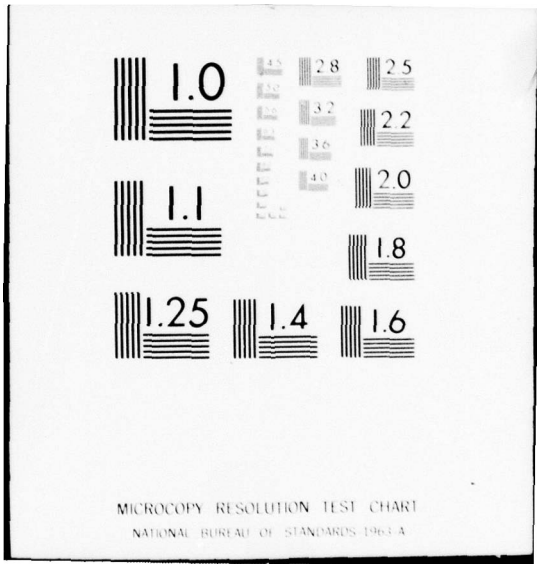
1.0
1.1
1.25
1.4
1.6
1.8
2.0
2.2
2.5
2.8
3.2
3.6
4.0
MICROCOPY RESOLUTION TEST CHART
NATIONAL BUREAU OF STANDARDS 1963-A

AFAPL-TR-77-71

(2)

HIGH OUTPUT SOLAR CELL WITH MULTILAYER AR COATING

OPTICAL COATING LABORATORY, INC.
PHOTOELECTRONICS DIVISION
INDUSTRY, CALIFORNIA 91746

NOVEMBER 1977

TECHNICAL REPORT AFAPL-TR-77-71
Final Report for Period August 1976 – August 1977

AIR FORCE AERO PROPULSION LABORATORY
AIR FORCE WRIGHT AERONAUTICAL LABORATORIES
AIR FORCE SYSTEMS COMMAND
WRIGHT-PATTERSON AIR FORCE BASE, OHIO 45433

NOTICE

When Government drawings, specifications, or other data are used for any purpose other than in connection with a definitely related Government procurement operation, the United States Government thereby incurs no responsibility nor any obligation whatsoever; and the fact that the government may have formulated, furnished, or in any way supplied the said drawings, specifications, or other data, is not to be regarded by implication or otherwise as in any manner licensing the holder or any other person or corporation, or conveying any rights or permission to manufacture, use, or sell any patented invention that may in any way be related thereto.

This report has been reviewed by the Information Office (OI) and is releasable to the National Technical Information Service (NTIS). At NTIS, it will be available to the general public, including foreign nations.

This technical report has been reviewed and is approved for publication.

Cecil Stuerke
Project Engineer

FOR THE COMMANDER

Joseph Wise

JOSEPH F. WISE, TECH MGR
Solar Energy Conversion
Energy Conversion Branch
Aerospace Power Division

"If your address has changed, if you wish to be removed from our mailing list, or if the addressee is no longer employed by your organization please notify POE-2 *,W-PAFB, OH 45433 to help us maintain a current mailing list".*

Copies of this report should not be returned unless return is required by security considerations, contractual obligations, or notice on a specific document.

AIR FORCE/56780/7 March 1978 — 150

Unclassified

SECURITY CLASSIFICATION OF THIS PAGE (When Data Entered)

REPORT DOCUMENTATION PAGE	READ INSTRUCTIONS BEFORE COMPLETING FORM
1. REPORT NUMBER: AFAPL-TR-77-71	2. GOVT ACCESSION NO.
3. RECIPIENT'S CATALOG NUMBER	
4. TITLE (and Subtitle): HIGH OUTPUT SOLAR CELL WITH MULTILAYER AR COATING	5. TYPE OF REPORT & PERIOD COVERED: Final Report, Aug 76 - Aug 77,
	6. PERFORMING ORG. REPORT NUMBER
7. AUTHOR(s): Peter Iles	8. CONTRACT OR GRANT NUMBER(s): F 33615-76-C-2166
9. PERFORMING ORGANIZATION NAME AND ADDRESS: Optical Coating Laboratory, Inc., 15251 E. Don Julian Road, City of Industry, CA 91746	10. PROGRAM ELEMENT, PROJECT, TASK AREA & WORK UNIT NUMBERS: 682J0404 P4
11. CONTROLLING OFFICE NAME AND ADDRESS: Aero Propulsion Laboratory POE, WPAFB, OH 45433	12. REPORT DATE: Nov 77
	13. NUMBER OF PAGES: 76
14. MONITORING AGENCY NAME & ADDRESS (if different from Controlling Office)	15. SECURITY CLASS. (of this report): Unclassified
	15a. DECLASSIFICATION/DOWNGRADING SCHEDULE

16. DISTRIBUTION STATEMENT (of this Report)

Approved for public release; distribution unlimited

63401F

17. DISTRIBUTION STATEMENT (of the abstract entered in Block 20, if different from Report)

18. SUPPLEMENTARY NOTES

19. KEY WORDS (Continue on reverse side if necessary and identify by block number)

Solar Cells
Antireflection Coating
Photovoltaics
Space Power

20. ABSTRACT (Continue on reverse side if necessary and identify by block number)

During this contract, high efficiency, polished surface, uncoated cells were prepared, and when AR coated with multilayers, achieved AMO cell output in the range 74-80 mW. These cells showed promise for space uses; additional work was identified to make these cells fully compatible with present methods for electrostatically bonding integral covers to cells.

DD FORM 1 JAN 73 1473 EDITION OF 1 NOV 65 IS OBSOLETE

Unclassified

SECURITY CLASSIFICATION OF THIS PAGE (When Data Entered)

410693

FOREWORD

This final report for contract F 33615-76-C-2166 was submitted by the Photoelectronics Division of OPTICAL COATING LABORATORY, INC. The effort was sponsored by the Air Force Aero Propulsion Laboratory, Aerospace Power Division under Project 682J, Task 682J04, Work Unit 682J0404. Lt. Cecil Stuerke was the Air Force Project Engineer, P. A. Iles was technically responsible at OCLI. The work covered the period August 1976 to August 1977.

TABLE OF CONTENTS

TABLE OF CONTENTS

- CONTINUED -

LIST OF FIGURES

LIST OF TABLES

SECTION I

PROGRAM OBJECTIVE

The objective of this program was to investigate multilayer coating techniques to achieve 15% efficient silicon solar cells for potential Air Force vehicle application. The investigation included determination of the compatibility of the cells with electrostatic bonding of coverslips and in demonstrating space environmental compatibility.

1. Overall Tasks

1) Theoretical and experimental evaluation of multilayer solar cell antireflection coatings was conducted to determine optimum materials and processing.

2) Cells fabricated according to the optimum design were optically and environmentally tested.

3) Compatibility of electrostatically bonded cover glass and optimized multilayer antireflection coatings was investigated.

4) Experimental and control cells were fabricated and delivered.

2. Technical Plan of Attack

The overall technical program can be summarized as follows:

1) Good output, uncoated violet-type cells were fabricated. Continuing tests were completed to optimize the properties of these cells for highest output with MLAR coatings, and also for best compatibility with the ESB cover process.

2) Various MLAR coating designs were generated and tested on the cells; these coatings involved two or more layers, and their relative performance and ease of manufacture was evaluated.

3) Regular deliveries of state-of-the-art cells were made.

4) The environmental performance of the cells and coatings was tested; the most promising cells were tested for their performance after ESB covers were applied.

5) A final shipment of the optimum cell-coating combination was made.

SECTION II

BACKGROUND TO CONTRACT

1. Recent Improved Solar Cells

In recent years, significant improvements have been applied to solar cells, in two main areas, namely:

1) The violet cell, (Reference 1). Here a shallow diffused layer of higher sheet resistance was combined with a close spaced grid pattern, adequately reducing the series resistance of this layer and yet comprising lines fine enough to maintain active areas in excess of 90% (i.e., > $3.6cm^2$ for $4cm^2$ cells). To ensure good output the front surface contact was made of metal combinations which did not degrade the PN junction, and lastly an improved antireflective coating, a single quarter-wave coating of Ta_2O_5 was used, providing good transmission in the short wavelength region where increased cell output was provided.

In most cases, the maximum power under AM0 illumination of such violet cells ($4cm^2$ area) fell in the range 70 to 76mW when covered with a quartz or glass cover.

2) The non-reflective form of the violet cell, (Reference 2). Here the major improvement resulted from the formation (by orientation preferential chemical etching) of a precisely textured surface, consisting of many small pyramids of height around 5 to 10 μm. The textured surface has very low reflectance (even more decreased by single layer AR coating). With suitable processing, these textured cells have had AM0 power output in the range of 78 to 85mW for $4cm^2$ cells.

The present work was intended to bridge the gap between cells 1) and 2) above, to provide cells with a smooth surface, but with output power between the best violet cells and textured cells.

2. Associated Technology

a. Improved AR Coating

The single layer quarter-wave coatings, (Ta_2O_5 or TiO_x) have been improved, in increased transmission; because of their higher refractive index, they allow increased cell output when the cell is covered (increases range from 1 to 4% depending on the properties of the AR coating). However, the average reflectance for polished silicon with such coatings is 6% over the part of the solar spectrum to which silicon cells respond (0.3 to 1.2 μm).

It is possible to reduce overall reflectance by adding more layers. Successful application of such multilayer antireflective (MLAR) coatings has been achieved (References 3, 4, 5, and 6 and in-house work at OCLI). The reflectance produced by a single layer can be reduced by 3-4% if two correctly applied layers are used, and even more if more than two layers are used. For the two layer case (DLAR), this means that violet cell output can be increased by up to 4%, raising the actual output to 73 to 79mW range. The advantages of multilayers are less for non-reflective cells, because surface texturing has already reduced the overall reflectance markedly, thus leaving less room for further reduction by the coating. Part of the impetus for the present work was the promise of cells with multilayer antireflective (MLAR) coatings, with output between the best violet cells and the output range achieved for textured cells. Although the potential

improvement was only up to 6%, there was considerable scope for careful isolation of the correct combination of coating materials, and suitable control of the coating properties and the layer thickness. Thus it was necessary to control the refractive indices, the precise thicknesses, and the absorption in the solar spectrum.

b. Integral Coatings

For Air Force purposes, integral coatings on solar cells can have potential advantages. A most promising method of application is the electrostatic bonding method (Reference 7). To date, this method has been applied to a variety of cell contacts and coatings, but generally for complete bonding, the cell surface had to be highly polished, and the grid height above this surface could not exceed $\sim$ 2 μm.

The requirement for high surface finish has led to difficulties in bonding to textured surfaces. Therefore the goal of the present work is to try and provide high output cells approaching the 80mW region, (with the aid of MLAR coatings) which are adaptable to electrostatic bonding of these covers. The other necessary property of the cells, namely a low grid contact profile will be one of the secondary tasks undertaken in this contract.

c. MLAR Coating Properties

The contract work defined suitable layer materials, and determined the degree of control needed to ensure optimum properties. The possibility of improving suitable process control to maintain these optimum properites in manufacturing environment was investigated. In addition, the environmental stability of these various coating combinations was tested.

SECTION III

TECHNICAL PROGRAM

The work performed is discussed under separate headings as follows.

1. Cell Fabrication

To achieve output in the range required in this contract called for a cell with very good performance before application of the coating. In particular the cell current had to be maximized, by use of a shallow diffused layer which provided a wide range of spectral output, by control of the grid pattern to reduce series resistance by effective coverage of the diffused layer, and also to reduce the shadowed (inactive) area. Also the cell voltage must be high (by attention to the metal combination used with the shallow surface layer) and the curve fill factor (CFF) must be high, again from careful reduction of parasitic series and shunt circuit components. In addition this basic cell structure must be matched to the MLAR under study, and must also remain stable under the conditions by which the MLAR, and later the cover, are applied.

The cell design involved using a range of diffusion conditions, front contact metals and gridline application methods to produce the best structure. Particular attention was paid to the grid parameters. First, theoretical estimates were made on the relative effectiveness of grids of reduced profile (of direct use in the evaluation of the ESB method). Next, practical methods were used, including both the use of shadow masks with fine slits, and of various photoresist methods to form fine-line patterns. Along with these gridline methods, suitable combinations of

metals were evaluated, again with the goal of obtaining maximum cell output after application of the MLAR coating.

This direct cell method led early in the contract to cells about 7% lower than the expected target, because both the CFF and the active area were low. Later the gridline methods were improved to remedy these deficiencies.

2. Antireflecting Coating

a. Theoretical Work

The actual design of an MLAR coating suited to use with high efficiency cells must involve the choice of materials of suitably matched refractive index (n) and computation of the optimum thicknesses of each material which will lead to reduced reflectance over the spectral range of interest. The theoretical design must take into consideration the spectral response of the cell to be coated, reasonable values of absorption for the layers, the detailed reflective properties of the doped semiconductor surface and also the medium which will terminate the MLAR coating. For present space applications, this outer layer is an adhesive layer ($n \sim 1.43$); however, for electrostatically-bonded cells, the coating must be matched directly to a glass (typically 7070, with $n \sim 1.5$). In the cell output range in this program careful balance of these properties was required to extract the most power.

These theoretical problems become more severe as the number of possible layers is increased; as more candidate materials become available, more uncertainty is introduced as to the correct values of refractive index and absorption to be used.

In practice, an iteration program was used. In this, a MLAR was designed, experimental work applied the layers to the specified thickness, and then the cell behavior and the reflective and transmissive properties of the MLAR were checked to see how close the theoretically assumed values were to the practical values. After analysis, the amended layer properties measured in practice were either fed back into the theoretical program, or else further experiments were designed and done, to attempt to produce properties closer to the theoretical values.

The approach in the present work emphasized the properties of the coated cells; i.e., the cell output and response were the main criteria of the quality of the MLAR.

A measure of the coating effectiveness was the ratio of I_{sc} measured in the OCLI solar simulator before and after coating. A ratio of 1.48-1.49 would indicate good agreement with the theoretical calculations. In fact ratios between 1.45 and 1.47 were obtained initially, but later higher ratios were obtained. In Section III-d below some correlation between theory and experiment is shown.

(1) Spectral Response of Uncoated Cells

Initially the computer program used the spectral response of a conventional uncoated cell characteristically with diffusion depth $\sim$ 0.3μm, and with fairly high donor doping levels in the diffused layer, both these factors reducing short wavelength response. Later in the contract work, spectral response data typical of the shallow junction $\leq$0.2μm and reduced donor concentration were used in the computer program; use of these data shifted the product curve of cell response times input photons (from the AMO

spectrum) towards shorter wavelengths, and therefore altered the optimum properties of the MLAR layer. In practice, however, these layer corrections were overshadowed by the problem of obtaining the required properties in all dielectric layers in the MLAR. Even for two layer coatings (DLAR) the slight variation in refractive index thickness and particularly in absorption caused greater changes than predicted theoretically from using more realistic spectral response data.

Figure 1 shows the absolute spectral response (mA/mW) of a conventionally - diffused uncoated solar cell; Figure 2 shows a similar plot for a violet-type diffused cell. When these two response curves are multiplied with the AMO spectrum (Figure 3), the product curves Figures 4 and 5 are produced. The usual approach for designing AR coatings is to attempt to minimize reflectance over the spectral region of most interest for the cell; for example to obtain *minimum reflectance* over the wavelength range shown in the product curve Figure 5, a quarter-wave AR coating with a reflectance minimum at the maximum of the product curve ($\sim$ 570nm) is selected. Figure 6(a) shows the reflectance curve of a QWAR coating of Ta_2O_5 on a violet cell; it can be seen that although the reflectance is reduced for the shorter wavelengths, there is still appreciable reflectance at the longer wavelengths (above 800nm); although application of a dielectric layer (an adhesive layer or a cover) will change the reflectance slightly (see Figure 6(b)) the same conclusions apply.

If a DLAR coating is applied, the reflectance is shown in Figure 7(a); here the reflectance is low at both short wavelengths and longer wavelengths The application of a dielectric layer reduces the overall reflectance as shown in Figure 7(b).

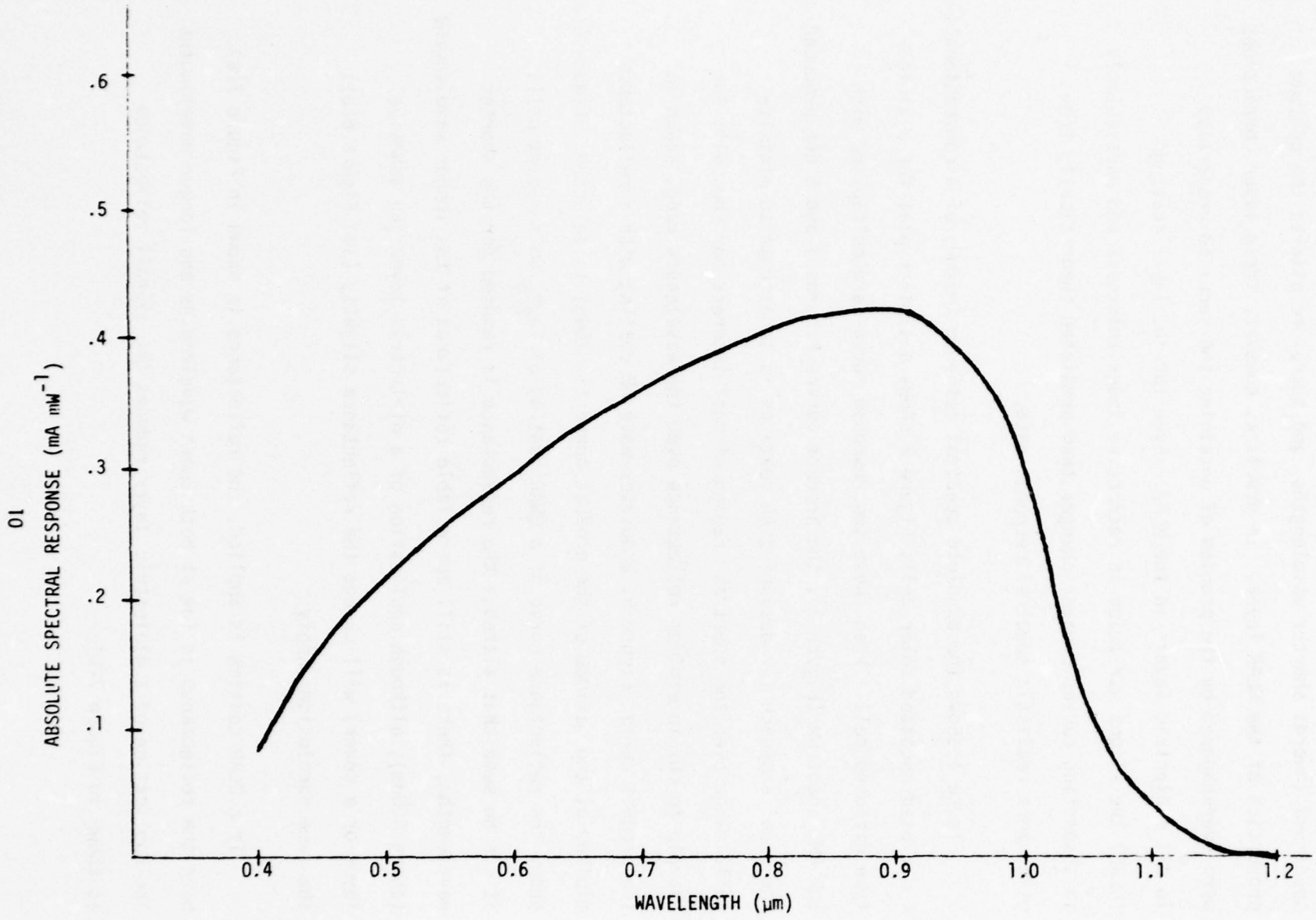

Figure 1: Absolute Spectral Response of Uncoated Conventional Cell

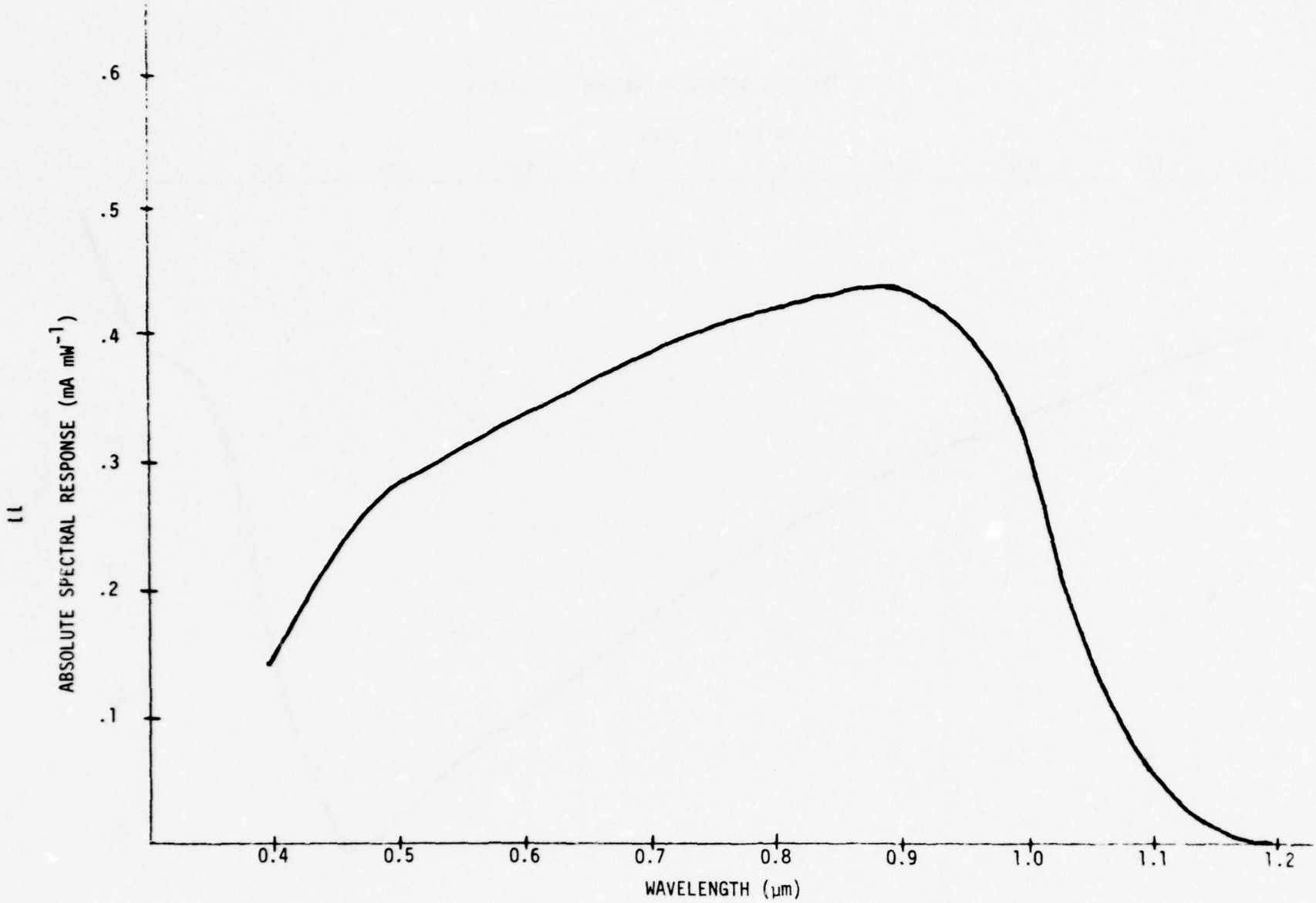

Figure 2: Absolute Spectral Response of Uncoated Violet Cell

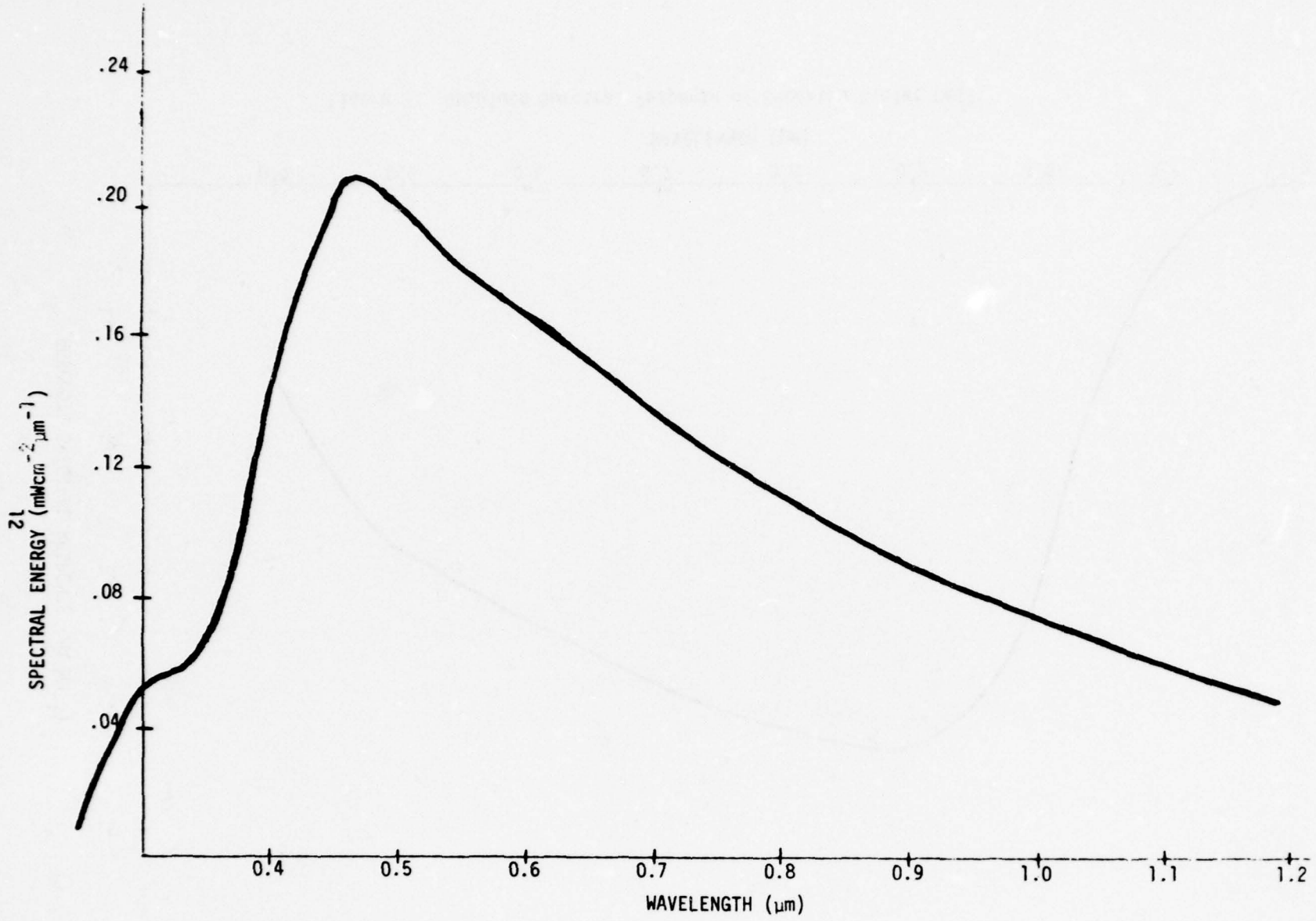

Figure 3: AMO Solar Output Spectrum

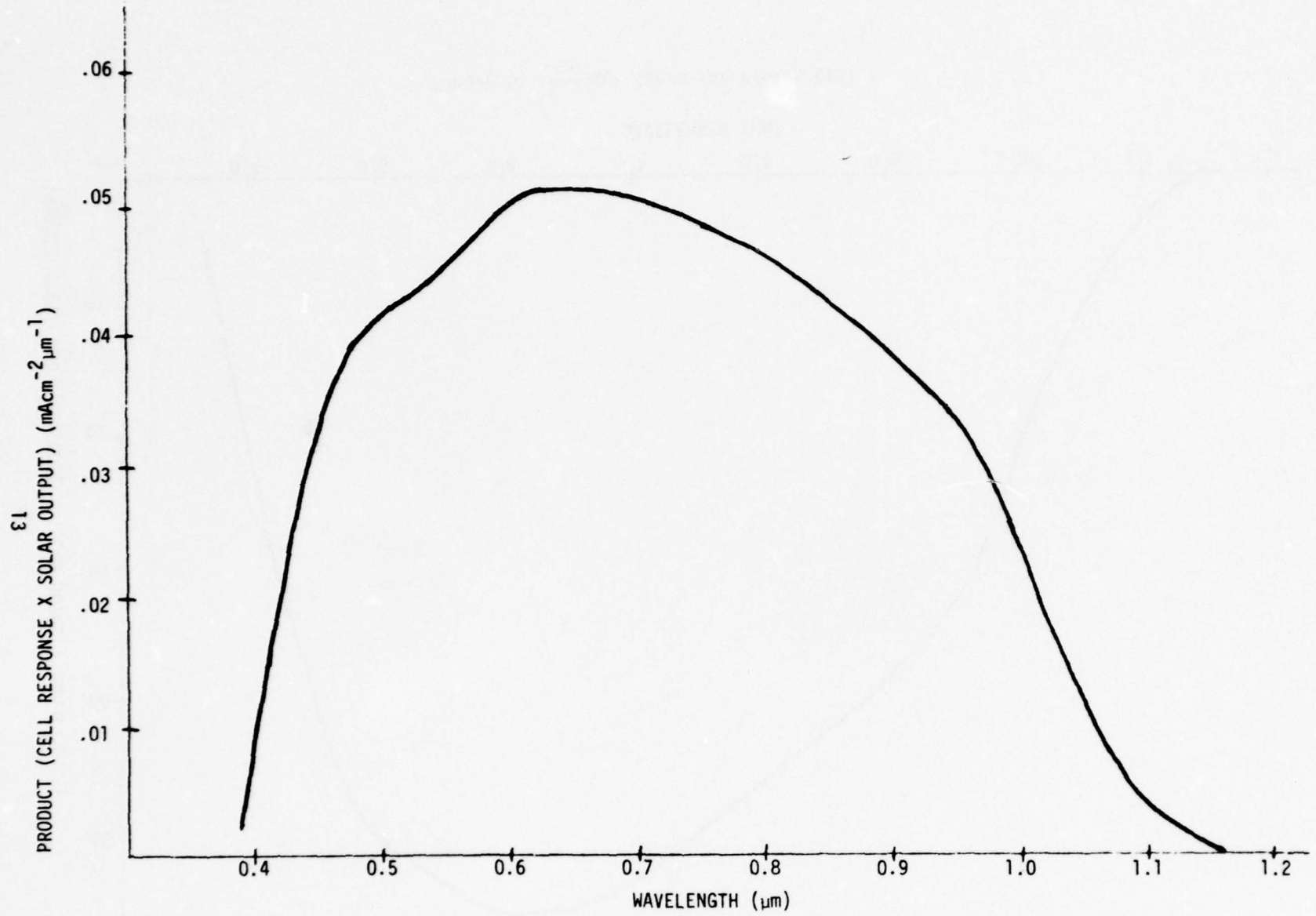

Figure 4: Product Curve for Conventional Cell

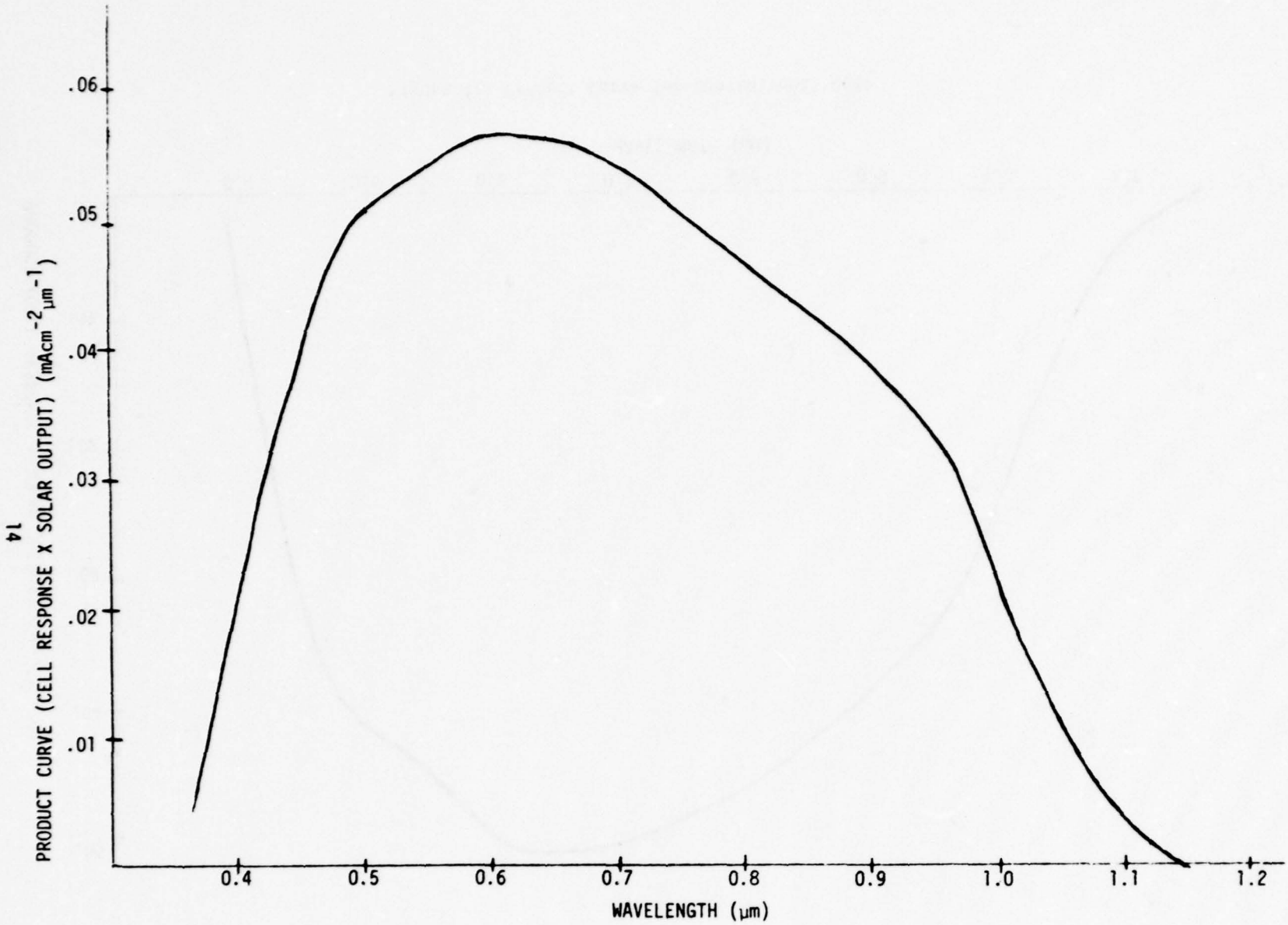

Figure 5: Product Curve for Violet Cell

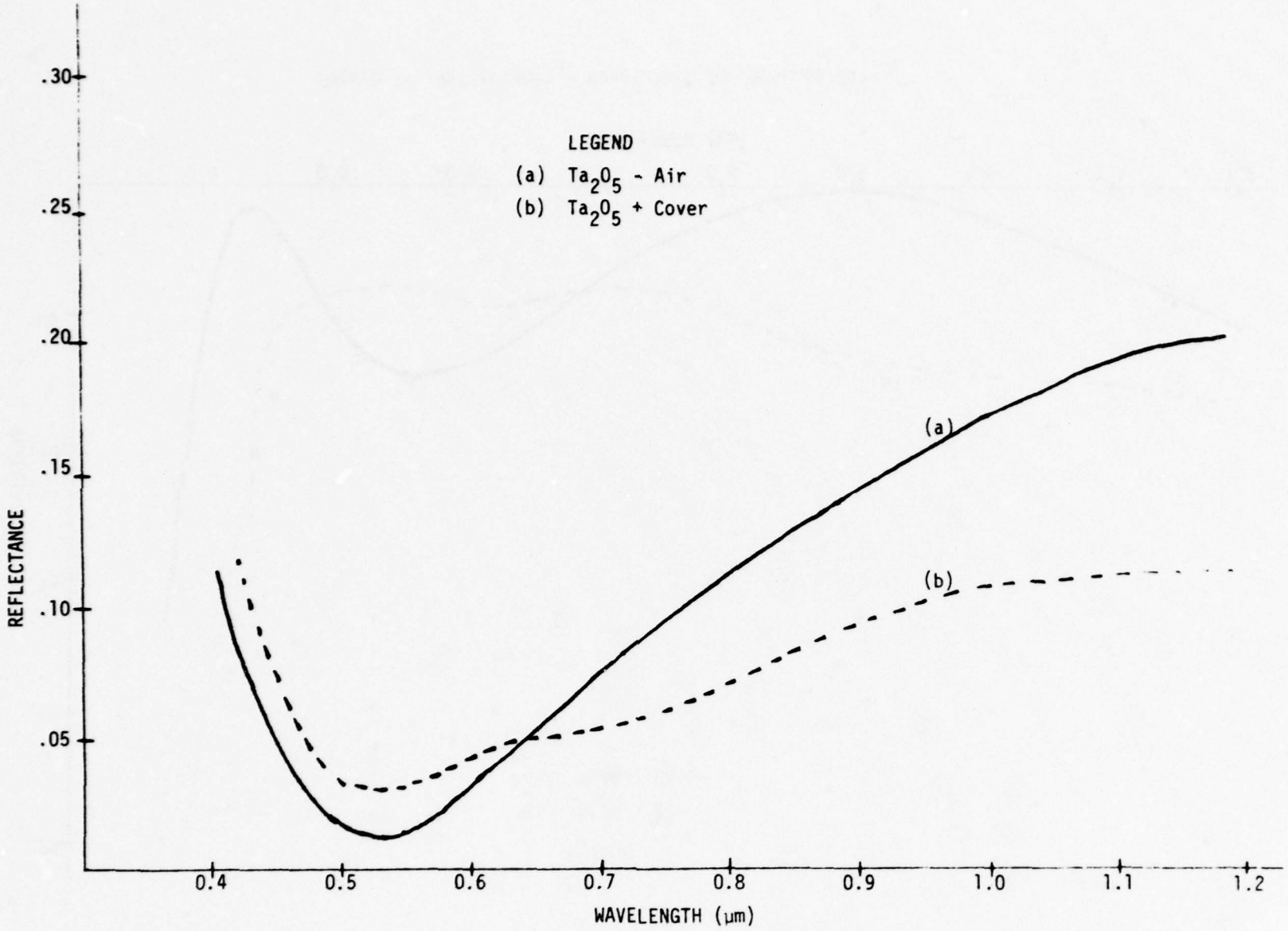

Figure 6: Reflectance - Wavelength for QWAR Ta_2O_5 on Cell

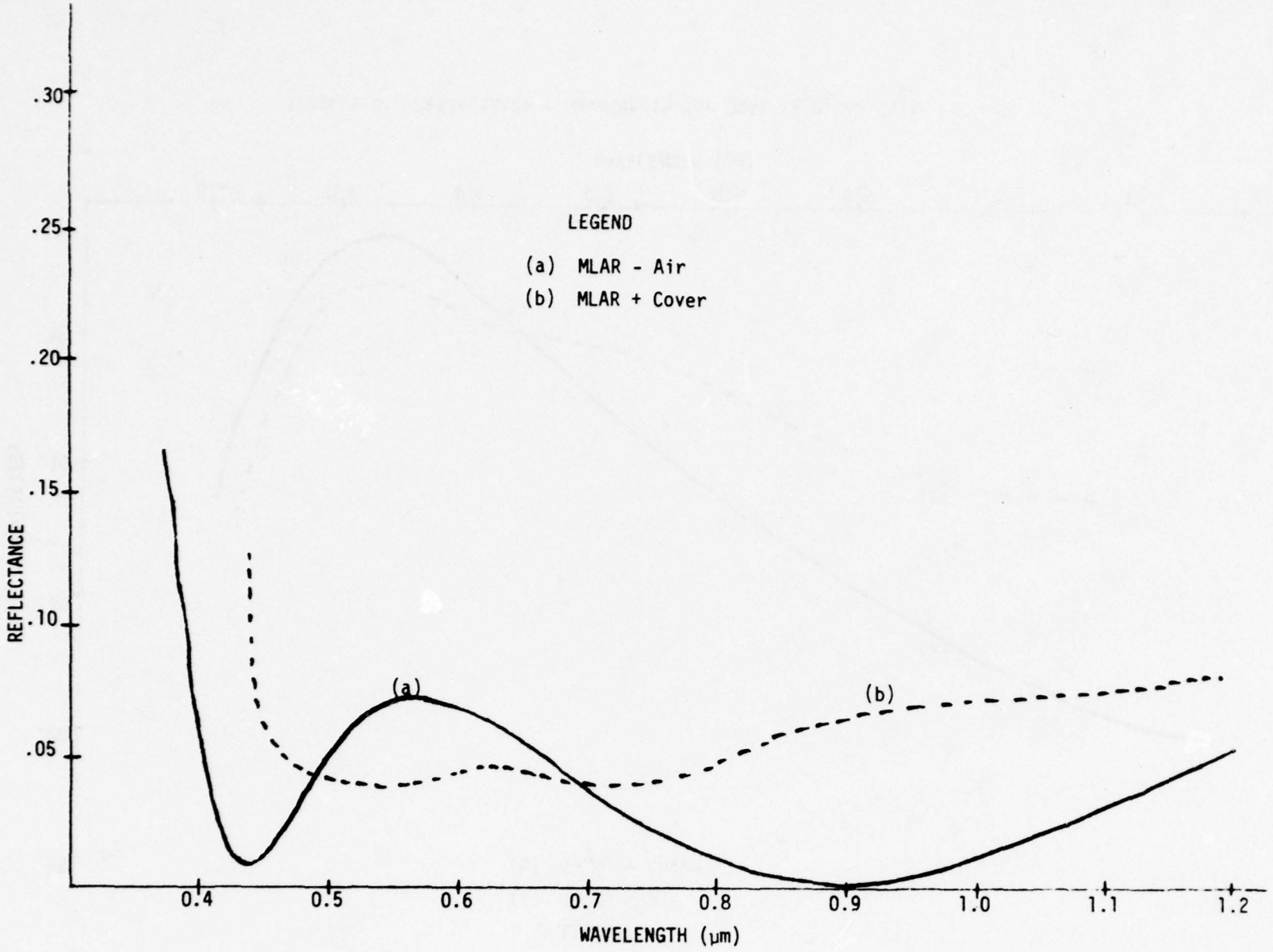

Figure 7: Reflectance - Wavelength for MLAR on Cell

(2) Effects of Varying Layer Thicknesses

The usual sequence for DLAR coating uses a high (H) refractive index layer ($n > 2.1$) applied to the silicon, followed by a lower (L) refractive index layer ($n \sim 1.6$-1.7) applied to the H-layer.

The baseline design assumes a QW thickness of each layer, and for this design the computed reflectance curve is as shown in Figure 7(a). Figures 8(b) and 8(c) show the effect on reflectance of an intentional 30% increase or decrease in the H-refractive index layer. In Figures 9(b) and 9(c) similar curves are shown for 30% variations in the L-layer, with 9(a) again showing the baseline design. These curves show that variations in the L-layer are more serious.

These conclusions differ when the L-layer is covered by a layer with n even lower than that of the L-layer (e.g., n=1.45 corresponding to the cover adhesives or testing oils used).

Figure 10(a) shows the baseline design (for correct layer thicknesses) for the dielectric-L-H-Si sequence; Figures 10(b) and 10(c) show the result of ±30% variation in the H-layer. Similarly Figures 11(b) and 11(c) show the effect of ±30% variation in the L-layer compared to the baseline in Figure 11(a). For these latter two cases, the two layers behave opposite from the air-terminated case, namely that variations in the L-layer are less serious.

These curves give an idea of how subtle variations in one controlled parameter, the layer thicknesses, can affect the reflectance, and thereby the solar cell output. In addition to thickness variations caused by

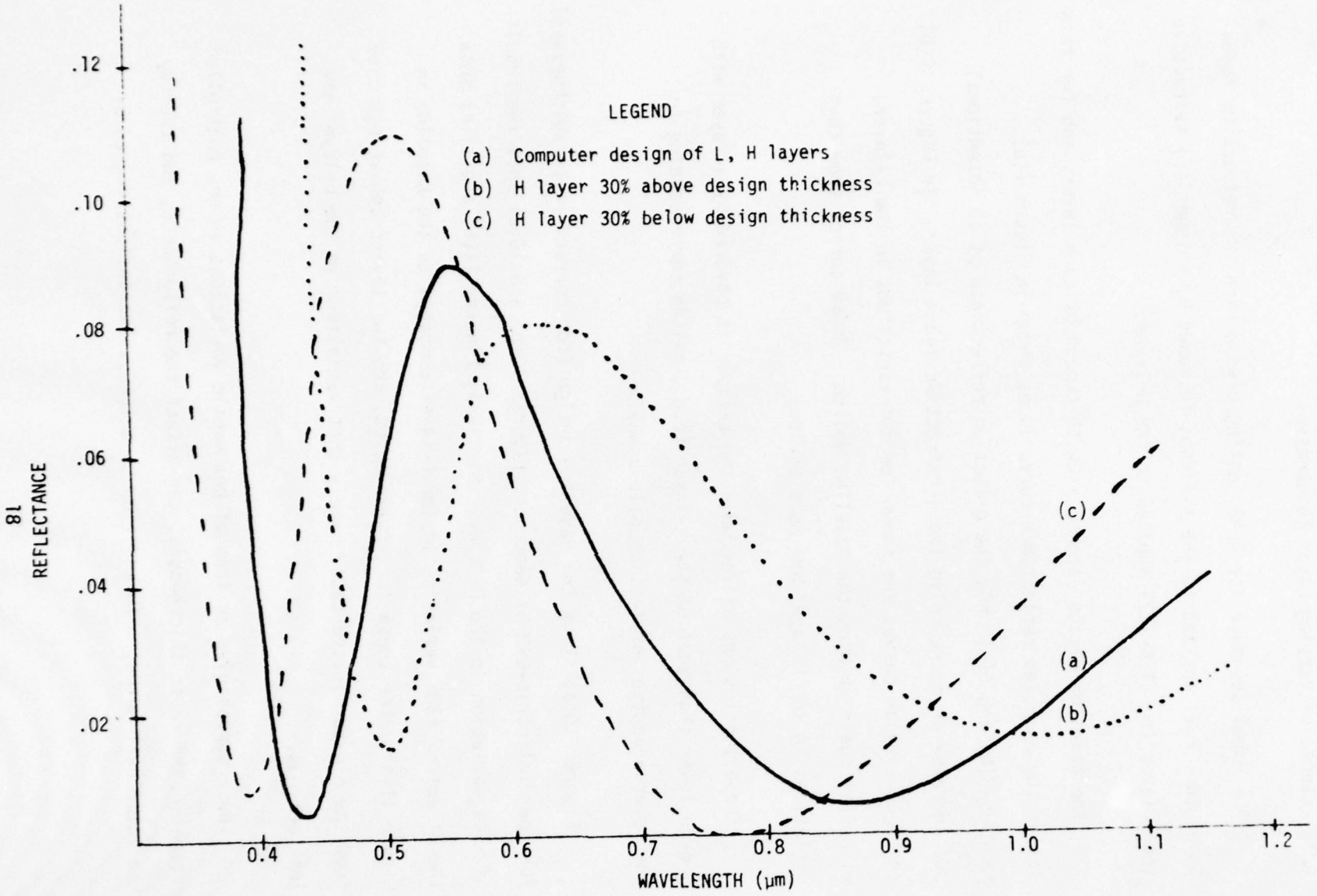

Figure 8: Reflectance - Wavelength for DLAR on Cell

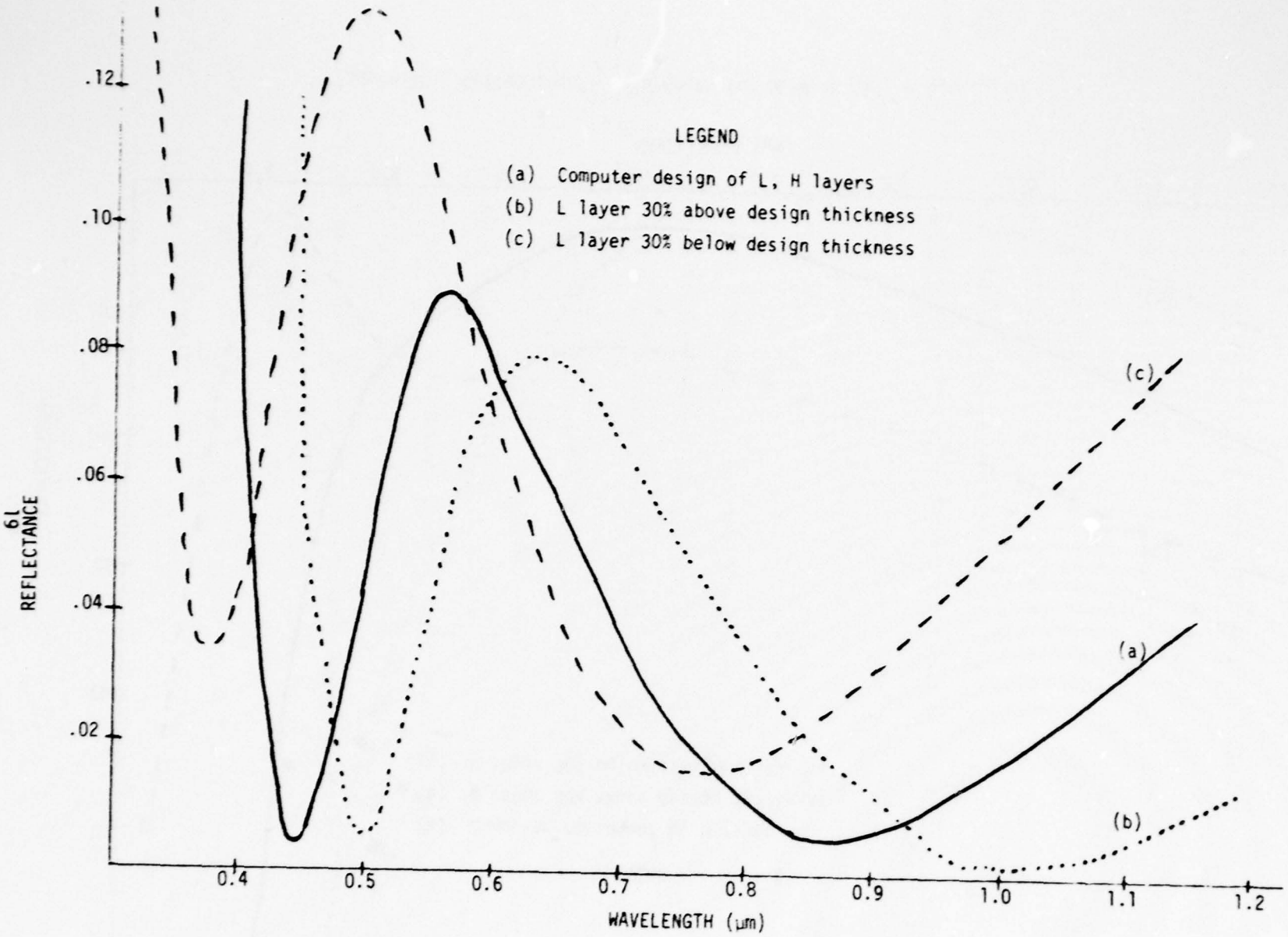

Figure 9: Reflectance - Wavelength for DLAR on Cell

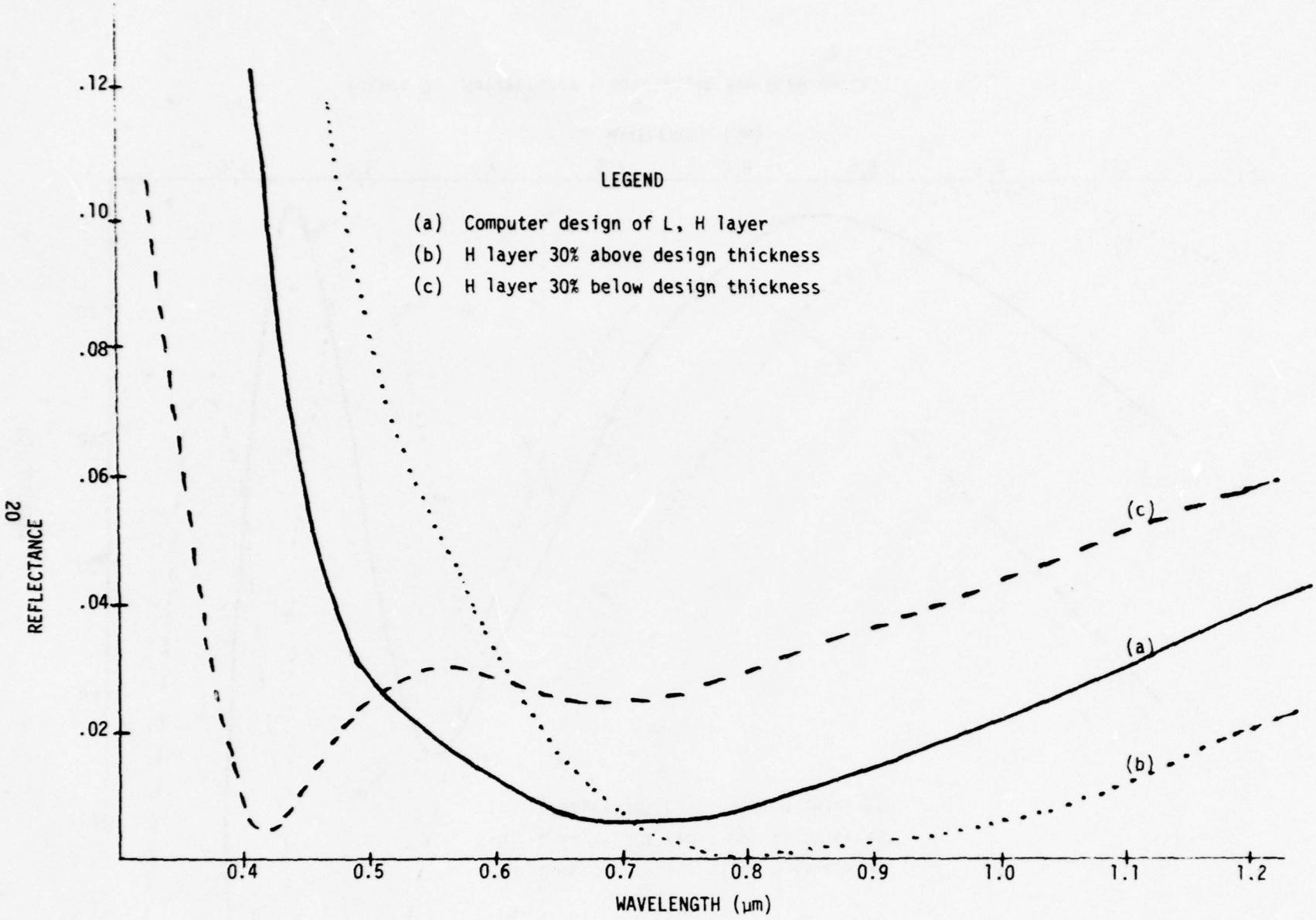

Figure 10: Reflectance - Wavelength for DLAR on Cell + Oil

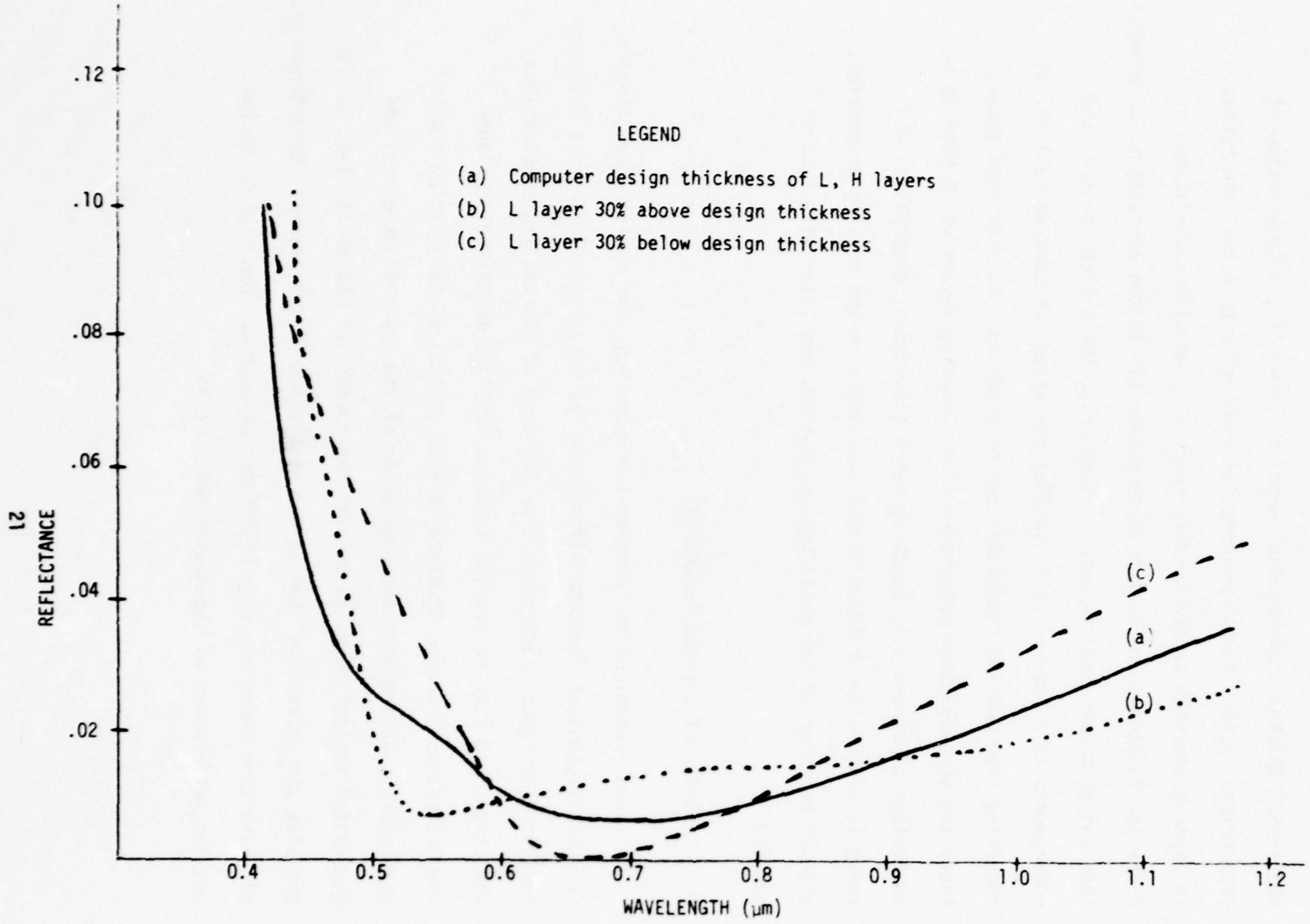

Figure 11: Reflectance - Wavelength for DLAR on Cell + Oil

slight monitoring differences, in most vacuum chambers, there will be additional thickness variations caused by "run-off", a combination of geometrical factors during evaporation combined with actual variations in layer properties caused by differences in deposition conditions at different locations on the substrate holder (including variations in temperature and/or background pressure). Similarly, the n=1.45 covered case corresponds to a covered cell, so that variations in covered cell output resulting from coating conditions can be expected. As mentioned above, there are several other properties of the coating layers which have to be controlled simultaneously (such as refractive index, absorption) and there is interaction between slight variations in the coating properties, and the behavior of the cells both as coated, and later with a cover applied.

b. Transfer of Coating Technology

It was convenient to transfer the technology for applying multilayers from OCLI/Technical Products Division to the OCLI/Photoelectronics Division facility, to reduce turnaround time for some of the coating combinations and tests, and also to provide a useful baseline throughout the work. The technology transfer involved careful control of the coating chamber parameters (particularly the monitoring of the layer thicknesses) and associated optical tests to confirm the success of the monitoring, and to evaluate the refractive indices and absorption of the layers. Repeatability of refractive index was very important, of course. The main criterion was the performance of the coated solar cells.

These chamber conditions which influence coating properties include variables such as the degree of vacuum obtained (i.e., the lowest pressure required), the type and pressure of the background gas introduced into the chamber, and the temperature maintained at the cells while they are coated. There are also other possible variables, including the possibility of outgassing from the chamber components (especially the source used for the layer materials) and the rate of deposition of the layers.

The goal of this contract was to determine repeatable processes wherein these variables were controlled to yield the required layer properties. The combination of experimental coating evaporators, and a manufacturing level coater at PED provided good estimates of possible difficulties in scaling-up the MLAR coating processes. A most important factor in coating application, is the "run-off" or maximum variation of coating properties obtained for samples of various locations in the chamber. Knowledge of the run-off can lead to possible reduction in variations, and can serve as a good guide for potential use of processes in a manufacturing environment.

These expectations were realized, and for much of the contract the MLAR coatings which achieved the goals of the contract were applied under conditions similar to those expected for manufacturing larger numbers of cells.

In order to provide 2x2cm cells with output higher than 76mW (14%), several stringent simultaneous restrictions are placed on the photovoltaic parameters:

(1) J_{sc}

The current density of the uncovered cell must be $\sim$ 42.5 mA/cm^2, and the active area must exceed 3.76cm^2 (94%).

(2) V_{oc}

Values above 600mV are required.

(3) CFF

Values above 0.78 are required.

These parameters were interrelated; for example, if the N+ diffusion cycle was adjusted to reduce the depth of the diffused layer, the increased sheet resistance reduced the CFF. If the gridline coverage (or grid conductivity) was increased to raise CFF, there was chance of reduced I_{sc}.

In practice, with careful control of the grid pattern coverage, bare cells were made with > 50mW output; when a MLAR coating was applied, the cell output increased to > 76mW. In shipping lot #3, eleven (11) of the twenty-two (22) MLAR cells shipped had output (uncovered) above 76mW (14.6%). The general level of output continued to improve (see discussion on cell shipments in Section IV). Also, as described in Section III-3 the cell fabrication process was varied in some tests, in attempts to provide increased compatibility with the ESB process.

c. AR Coating Tests

The sequence of tests used to optimize the coatings was as follows:

1) The separate coating materials were selected on the basis of their theoretical or earlier-known properties. Possible candidate materials for the H-layer were Ta_2O_5 or TiO_x; for the L-layer, Al_2O_3, SiO, ZrO_2 were among the possible materials.

2) Quarter-wave coatings were deposited on quartz and silicon; reflectance curves were run, and from these curves, the refractive indices, and optical thicknesses could be measured. In some cases the absorptance could be deduced from the reflectance curves. The coating chamber variables were varied systematically to approach the theoretical properties, the layers were combined and reflectance curves run with both air - and oil terminated conditions.

3) Next these combined coatings were applied to uncoated cells, and comparison of cell output before and after coating showed the effectiveness of the coating. As mentioned earlier, evaluation of cell performance was given prime importance.

4) On analysis of the separate coating layers, and of the cell behavior, iterative tests were run to improve the coating properties.

5) Different coating properties were tried; e.g., for Ta_2O_5, different evaporation conditions (source materials, background oxygen pressure etc.) can give a range of refractive index (2.1 to 2.3) and also varying absorptance. Similar variations could be made in the L-layer properties.

A special case tested was the variation in substrate (silicon) temperature during the evaporation of TiO_x. Section d below discusses the results of some of these coating variations.

6) Later in the contract when possible moisture effects were found, some additional variations were made of the addition of an intentional optically thick layer of a low-n layer such as SiO_2 or MgF_2 (see Section V-5).

d. Results of Some Coating Variations

Several different combinations were used to illustrate the methods used to select the best MLAR coating conditions.

1) For DLAR with the H-layer Ta_2O_5 of $n \approx 2.2+$, and L-layer Al_2O_3, the thickness of the Ta_2O_5 layer was varied systematically from 570Å to 670Å and cell reflectance and I-V measurements made. Afterwards a layer of Al_2O_3 was applied, and the same cell parameters measured. Cells with three different Ta_2O_5 thicknesses (570Å, 620Å and 670Å) are shown in Figure 12. The reflectance versus wavelength curves are shown for Ta_2O_5 and Ta_2O_5 plus Al_2O_3, Also Table 1 shows the AMO I_{sc} values (including long wavelength and short wavelength contributions) before and after the addition of the L-layer. The results show that the thinner layers of Ta_2O_5 (nearer to the theoretical values) were slightly better.

2) A test similar to 1) wherein SiO ($n \sim 1.9$, thickness $\approx$ 750Å) was applied over Ta_2O_5. In this case the DLAR reduced the cell I_{sc} below its QWAR value (Table 2); despite some increase in long wavelength response (caused by reduced reflectance) the predominant effect was severe reduction in short wavelength response, probably from absorption in the SiO layer.

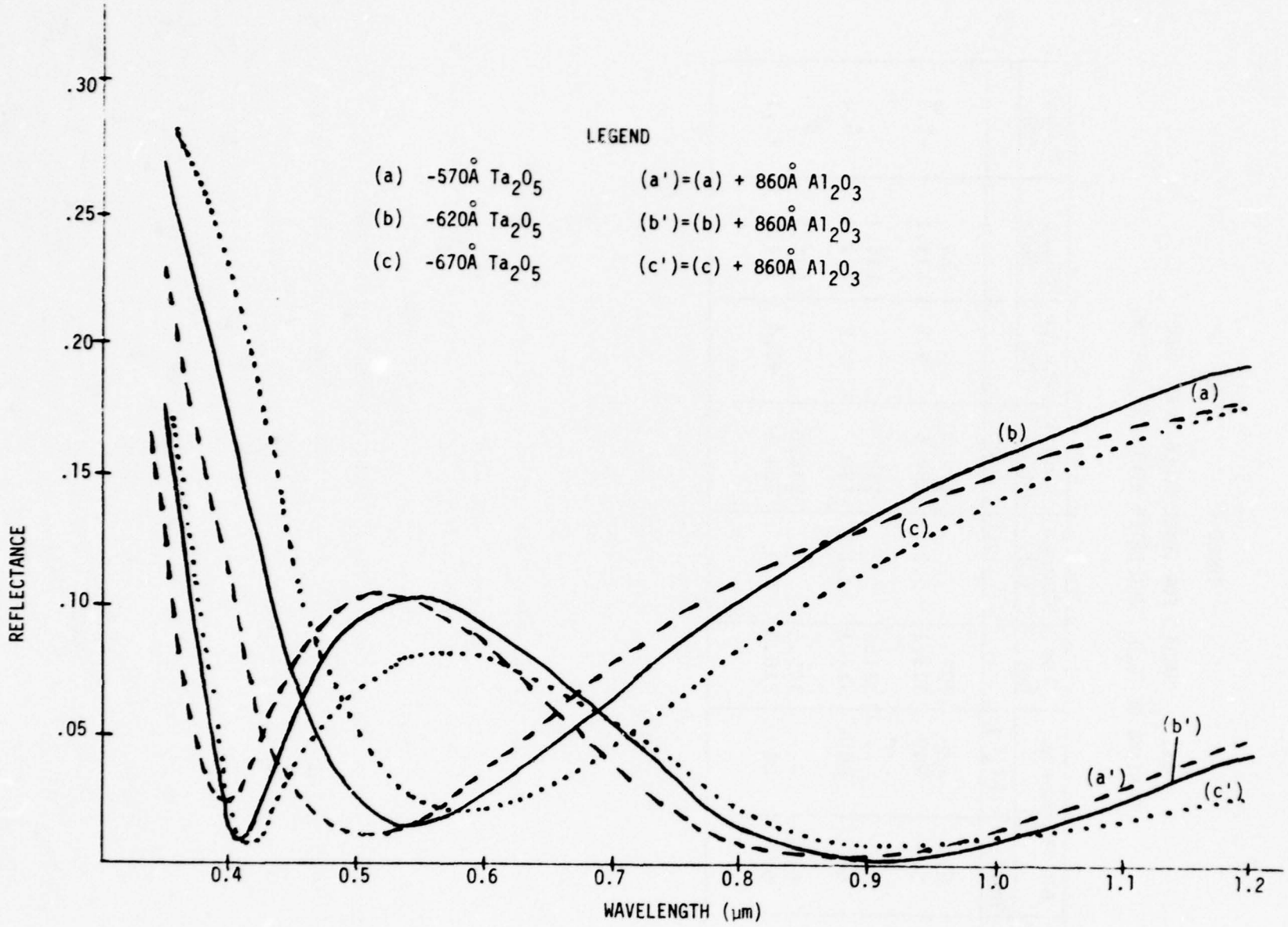

Figure 12: Reflectance - Wavelength for QWAR Ta_2O_5 on Cell ± Al_2O_3

TABLE 1

AMO I_{sc} VALUES FOR THREE CELLS, WITH QWAR COATING OF Ta_2O_5, AND LATER WITH DLAR COATING

Cell #	AR Thickness (Å)		Isc (mA)	Change (%)	Long λ (mA)	Change (%)	Short λ (mA)	Change (%)
	Ta_2O_5	Al_2O_3						
14	570	---	307		172.4		135	
	570	860	323.1	+5.2	189.6	+9.9	133.1	-1.5
9	620	---	311.6		177		135.1	
	620	860	322.1	+3.3	188	+6.2	134.6	-0.4
11	670	---	309.5		178.5		131.3	
	670	860	316.8	+2.3	184.6	+3.4	134.1	+2.1

TABLE 2

AMO I_{sc} VALUES FOR CELLS WITH Ta_2O_5 COVERED BY SiO

Cell #	AR Thickness (Å)		Isc (mA)	Change (%)	Long λ (mA)	Change (%)	Short λ (mA)	Change (%)
	Ta_2O_5	SiO						
1	600	---	311		173.5		137.1	
	600	750	305	-2	187.6	+8	117.5	-14.5
6	600	---	308.6		176.6		132.6	
	600	750	295.2	-4.5	183.2	+3.8	112.8	-15
18	600	---	314.2		184.2		130.4	
	600	750	300.6	-4.5	186.6	+1.3	114.5	-12.2

3) In another series of tests, various Al_2O_3 layer thicknesses between 760 and 1025Å were applied over Ta_2O_5-coated cells. These Al_2O_3 layers were deposited without substrate heating, or high background pressure of oxygen, and although they had adequately reduced reflectance, their absorpiton reduced I_{sc}. Figure 13 shows the variation in I_{sc} as a function of Al_2O_3 thicknesses, with corresponding curves for the changes in long and short wavelengths. Also shown underneath are the reflectance values and wavelength positions of the two minima in the R-λ plot for air termination.

4) Another test was run to deposit TiO_x at higher substrate temperatures (250, 300, 350 and 400°C) in attempts to increase the refractive index of TiO_x used as the H-layer. A high n-value was obtained but these tests were discontinued because the combination of these high temperatures and the relatively high background pressure of oxygen during evaporation caused degradation in the coated cell characteristics, apparently from contact deterioration. As the substrate temperature was increased, the four cell groups showed serious CFF losses (0/4 at 250°C, 1/4 at 300°C, 2/4 at 350°C and 4/4 at 400°C). Thus this did not appear a promising approach to attempt to improve the normal H-L coating stack because the potential cell losses from CFF reduction were much larger then the sought-for gain.

e. Cover Tests

Section III-2a discussed the theoretical model wherein the MLAR layers were designed with the assumption that the coating stack was terminated in a dielectric of refractive index around 1.45-1.55 (corresponding

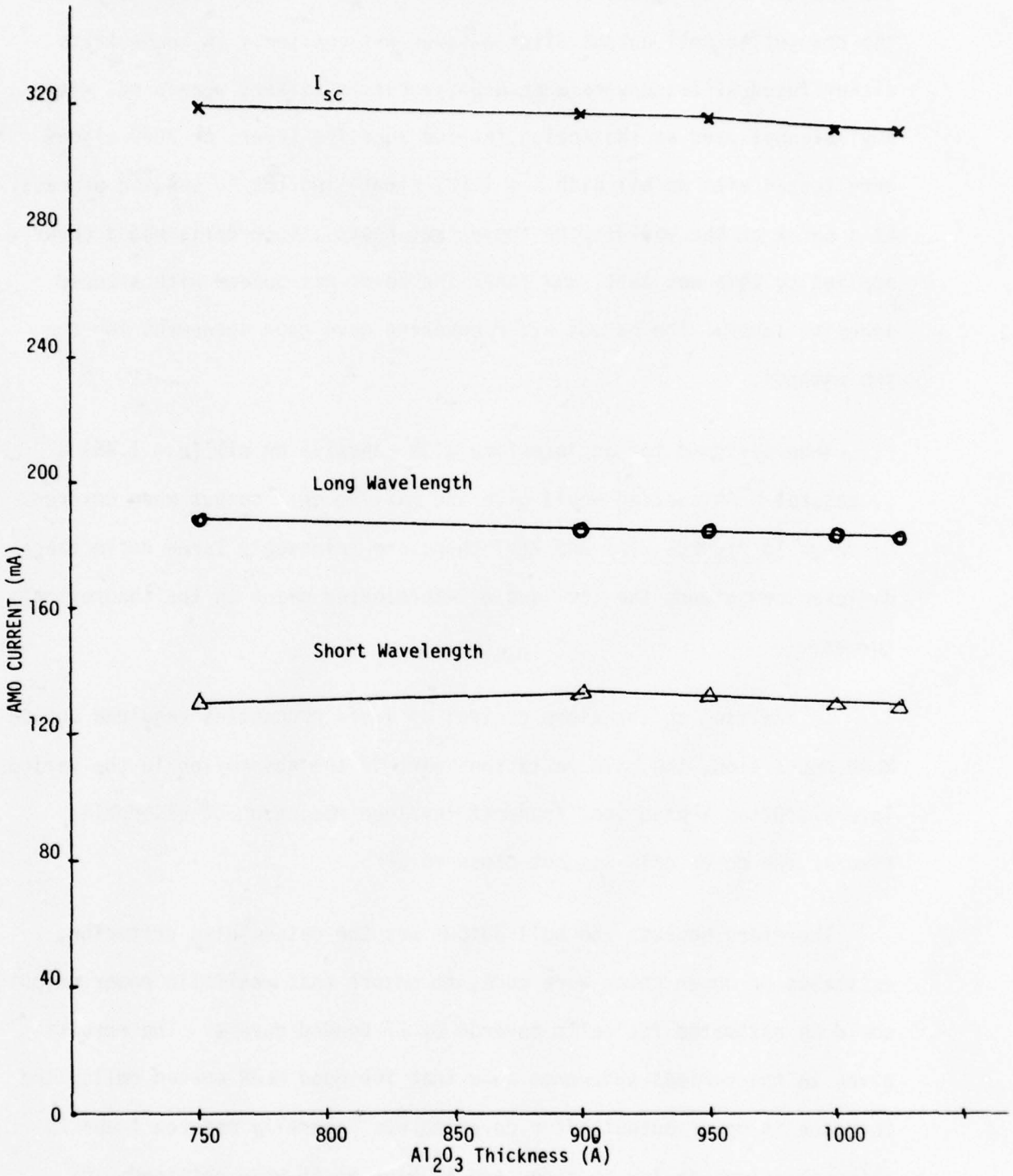

Figure 13: AMO I_{sc} Variation Versus Thickness of Al_2O_3 (low n) Layer

to the usual practical cases for an adhesively-bonded cover). Thus, the evaluation of the MLAR coated cells included sample readings of the changes in cell output after a cover was applied. In these tests either fused silica covers with a 350nm cut-on filter, were used, with amyl alcohol used as the analog for the adhesive layer; or 7070 slides were tested with an oil with $n \approx 1.52$, simulating the ES bonding process. As a check on the validity of these "wet tests", some cells had a cover applied by this wet test, and later the cover was bonded with a cured adhesive layer. The output after covering gave good agreement for the two methods.

When designed for an interface with adhesive or oil ($n \sim 1.45$) a successful MLAR coating would give the maximum cell output when covered. As shown in Figures 7(a) and 7(b) there are relatively large reflectance differences between the air- and oil-terminated cases in the theoretical curves.

In addition to the close control of layer properties required during MLAR deposition, the main variations were in the absorption in the various layers. Often a practical tradeoff involved reduction of absorption even if the cover gain was not close to zero.

Therefore because the cell output was the determining criterion, estimates of cover gains were made, to ensure that realistic power outputs could be estimated for cells covered by ES bonded covers. The results given in the various shipments show that for good MLAR coated cells, the increase in power output after covering was generally between 1 and 2% although values as low as zero, and as high as 4% were obtained. Of

most practical use was the actual power output after covering, because this output included gains following application of the coating, and the cover.

f. Heat Treatments

For all high efficiency silicon cells a heat treatment is usually required for several reasons, including reduction of contact resistance, improved adhesion of contacts to silicon, and improved adhesion and optical properties of the AR coating. In the present program, despite careful control of deposition conditions it was generally found advantageous to add a heat treatment after the MLAR was applied; this heating, in addition to improving coating adhesion and resistance to moisture attack also reduced the absorption in the multilayers. The coating deposition itself included a modest heat-cycle (up to 250°C) but often combined with a relatively high background oxygen pressure ($\sim 10^{-4}$ Torr). This latter heat cycle had adverse effects on some of the contact structures used. Therefore the best procedure involved.

1) A moderate heat treatment (500°C - 5 minutes in H_2) of the contacts before AR coating; this HT was useful both for improving contact adhesion, and also for reducing contact resistance sufficiently to allow uncoated cells to be selected above a minimum electrical output (typically > 50mW). Also this HT of the bare cell gave a reliable baseline output from which true coating gains could be measured.

2) Maintaining the HT (250°C - 45 minutes) during coating.

3) An additional HT like (1).

Some of the optical measurements made on the separate coating layers showed that post-evaporation heat treatment had opposite effects on the multilayers. For example, HT of the H-layer (first applied) often increased the absorption, whereas HT of the L-layer could reduce absorption in this layer. These opposed effects led to some confusion in evaluating tests of HT schedules. Typical results obtained in HT tests are shown in Tables 3 and 4. In Table 3 the opposed changes in short and long wavelengths can be seen. In Table 4 HT effects on various MLAR coated cells are shown; the results showed more dependence on contact variations than AR coating differences. Also the direction of change after HT did not favor breaking the evaporation sequence between layers and performing separate HT on each layer, because the H-layer is always present when the L-layer is heated. Therefore the compromise HT shown in 3) above was selected, and the results obtained towards the contract end showed that residual absorption could be reduced to a satisfactory level.

The HT scheduled used to make the cell also have impact on the ESB compatibility. The ideal cell HT would maximize output for the coated cell and would provide a built-in capability to withstand the full ESB conditions. A less favorable HT would maximize cell output, and would still remain below the threshold for failure when subjected to ES bonding.

Preliminary ESB tests showed that cells with high output did not withstand the additional HT required for ES bonding. At present, it appears that this failure mechanism was mostly from contact interaction, and it seems reasonable that improvements in the contact choice and structures will allow the several heat treatments needed to ES bond a cover to the

TABLE 3

HT (500°C - 5 MINUTES - H_2) TEST ON DLAR CELLS
(Ta_2O_5 - WITH VARYING THICKNESS OF Al_2O_3)

Ta_2O_5 Thickness (Å)	Al_2O_3 Thickness (Å)	Before (B) or After (A) HT	Isc (mA)	%	Long λ (mA)	%	Short λ (mA)	%
600	750	B	319.4		188.4		131.4	
		A	311.2	-2.5	184.4	-2.2	127.2	-3.2
600	900	B	315.8		183.7		132.5	
		A	318.1	+0.7	185.6	+1	133	+0.4
600	900	B	319		186.5		133	
		A	316.4	-1	187.4	+0.4	129.3	-2.8
600	930	B	301.3		177.2		124.6	
		A	297.8	-1.2	177.7	+0.3	120	-3.7
600	950	B	311.5		182.3		129.4	
		A	312.4	+0.3	184.6	+1.2	127.8	-1.2
600	1000	B	311.3		182		129.7	
		A	311.2	-0-	183.3	+0.7	128.3	-1.0
600	1025	B	315.5		184.6		131.6	
		A	315	-0.2	186	+0.8	128	-2.7

TABLE 4

HT EFFECTS ON CELLS WITH VARIOUS AR COATING COMBINATIONS

HT 600°C - 3 1/2 MINUTES - H_2

Cell #	AR Coating	Before (B) or After (A) HT	Voc mV	Isc mA	%	Long λ mA	Short λ mA	I_{500} mA	P_{500} mW	%	Comments
a	TiOx-Al_2O_3	B	601	314.6		182.8	132.1	292.2	146.1		2x4cm
		A	606	318.7	+1.3	184.9	134.2	294.8	147.4	+0.9	
b	"	B	599	319.3		185.7	133.6	285.3	142.6		"
		A	604	323.7	+1.4	188.1	136.1	296.8	148.4	+4	
c	"	B	603	320.2		186.8	133.8	257.3	128.6		"
		A	539	325.2	+1.5	188.6	137.1	59.1		Failed	
d	"	B	605	314.4		183.6	131.1	281.7	140.8		"
		A	561	319.1	+1.4	185.1	134.3	110	55	Failed	
e	"	B	602	321.1		186.9	134.5	267.7	133.8		"
		A	482	326.4	+1.6	189.7	137.3	-----	-----	Failed	Cr on FC
f	Ta_2O_5-Al_2O_3 (cold)	B	603	148.7		87.9	61.1	142.2	71.1		2x2cm
		A	606	151.2	+1.7	90.1	61.3	146	73	+2.7	
g	Ta_2O_5-Al_2O_3 (hot)	B	599	149.6		89.1	60.7	138.6	69.8		"
		A	601	134.8	-10	82.4	52.7	122.3	61.1	-12.5	
h	"	B	599	148.8		88.8	60.3	142.1	71		"
		A	600	136.1	-9	82.9	53.3	130.7	65.3	-8	

TABLE 4 (Continued)

HT EFFECTS ON CELLS WITH VARIOUS AR COATING COMBINATIONS

HT 600°C - 3 1/2 MINUTES - H_2

Cell #	AR Coating	Before (B) or After (A) HT	Voc mV	Isc mA	%	Long λ mA	Short λ mA	I_{500} mA	P_{500} mW	%	Comments
i	Ta_2O_5-Al_2O_3 (cold)	B	597	144.9		86.5	58.7	131.5	65.7		2x2cm
		A	600	147.2	+1.6	87.8	59.7	135.1	67.5	+2.7	
j	"	B	596	147		87	60.1	129.4	64.7		"
		A	597	151.2	+2.8	89.2	62.2	122.8	61.4	-5.2	
k	TiOx-Al_2O_3 (hot)	B	602	160.4		94	66.6	142.4	71.2		"
		A	608	162.6	+1.4	95.4	67.3	147.8	73.9	+3.8	Ta on FC
l	"	B	598	155.8		91.8	63.9	143.5	71.7		2x2cm
		A	604	157.7	+1.2	93.2	64.6	148.5	74.2	+3.5	
m	"	B	599	151.9		89.5	62.4	141.5	70.7		"
		A	604	153.3	+0.9	90.6	62.8	143.8	71.9	+1.7	
n	Ta_2O_5-Al_2O_3 (hot)	B	602	146.4		90.7	56	136.4	68.2		"
		A	602	146.4	-0-	91.3	55.3	128	64	-6.2	
o	TiOx-Al_2O_3 (cold)	B	603	151.5	151.	88.3	63.3	141.8	70.9		"
		A	606	152.7	+0.8	89.4	63.7	139.4	69.7	-1.7	
p	"	B	602	153.3		89.8	63.8	135.1	67.5		"
		A	603	155.2	+1.2	90.8	64.5	129.2	64.6	-4.3	Cr on FC

cell. This contact problem (as mentioned in Sections VI and VII below) was identified as the most urgent area for future study.

g. Comments on AR Coatings

The situation with the AR coating studies performed can be summarized as follows:

1) Successful deposition techniques were identified and developed to apply MLAR coatings with good coating gain ($\geq$ 1.48) to bare cells of good output; this coating could be performed under production-type conditions.

2) The deposition and post-deposition heat treatments maintained good cell output.

3) The AR coatings appeared to have good environmental performance (sometimes with slight attack by moisture) and 7070 covers could be ES bonded directly to the coating.

4) The cell output still increased $\sim$ 1-2% when a cover was applied.

5) In addition to decreased reflectance over most of the spectral range of interest (see Figure 7(a)), the reflectance at shorter wavelengths (below 450nm) was also decreased, and additional cell output in this spectral range leads to increased resistance of cell output to charged particle radiation damage.

3. Electrostatic Bonding (ESB) Compatibility Tests

In addition to providing potentially space-worthy cells of high output with MLAR coating, the contract was directed towards including

the capability of providing a stress-free integral cover by ES bonding. For successful combination with the ESB process, several guidelines were available at the beginning of the contract. These guidelines were:

1) The grid structure should have fairly low projection above the cell surface ($\leq$ 2μm) to allow conforming of the cover with the gridline after bonding.

2) There should be minimum stray metal between gridlines again to ensure good area coverage.

3) The cell must retain high active area, and good CFF, thus restricting the range of tradeoffs available from altering the grid pattern.

4) The cell should maintain high output after the heating cycle required for ES bonding. These requirements will be discussed in turn.

a. Low Grid Contact Profile

The limit quoted above ($\sim$ 2μm) was altered during the contract period, because SPIRE improved their ESB technology. These improvements increased the pressure applied to the cover during bonding, and thus aided deformation of the cover over surface protrusions such as the contacts. This addition reduced the need to try and place grooves in the covers to allow the cover to be placed over the contacts, and yet provide close approach of the cell and cover surfaces for good ES bonding. In addition the lower deformation possibility reduced the harmful effects arising from stray metal between the required pattern.

However, although the added pressure helped to deform the cover, the temperature-time cycle needed was still severe; thus if the grid height was too high, even with pressure and high voltage applied to the cover, a fairly severe heating schedule was required to complete a satisfactory bond. Thus high grid profiles still posed probelms. Several methods for reducing the profile were tried during the contract, as follows:

1) One way to reduce grid profiles is to decrease the grid spacing (i.e., more lines/cm) while maintaining narrower lines, to help achieve adequate active area. Some cells of this type were delivered in shipping lot #3, but already they showed that there was difficulty in maintaining both the active area and curve fill factor necessary to meet the contract goals.

Analysis of the grid pattern resistance shows the difficulty in trade-offs involved.

Consider cell and grid pattern of dimensions shown in Figure 14. The combined grid pattern losses can be expressed as a fraction of the load resistance for maximum power output of the cell. This load resistance $= 0.9 \frac{V_{oc}}{I_{sc}} = 0.9Z$. $R_{\square}$, $r_{\square}$ are used to designate the sheet resistances of the surface layer and grid metals, respectively. The fractional additive loss terms for the grid pattern are:

$$\frac{R_{\square} d^2}{8BL(0.9Z)} + \frac{r_{\square} Bd}{2WL(0.9Z)} + \frac{W}{d+W} \qquad (1)$$

SHEET RESISTANCE TERM

GRIDLINE RESISTANCE TERM

SHADOWING TERM

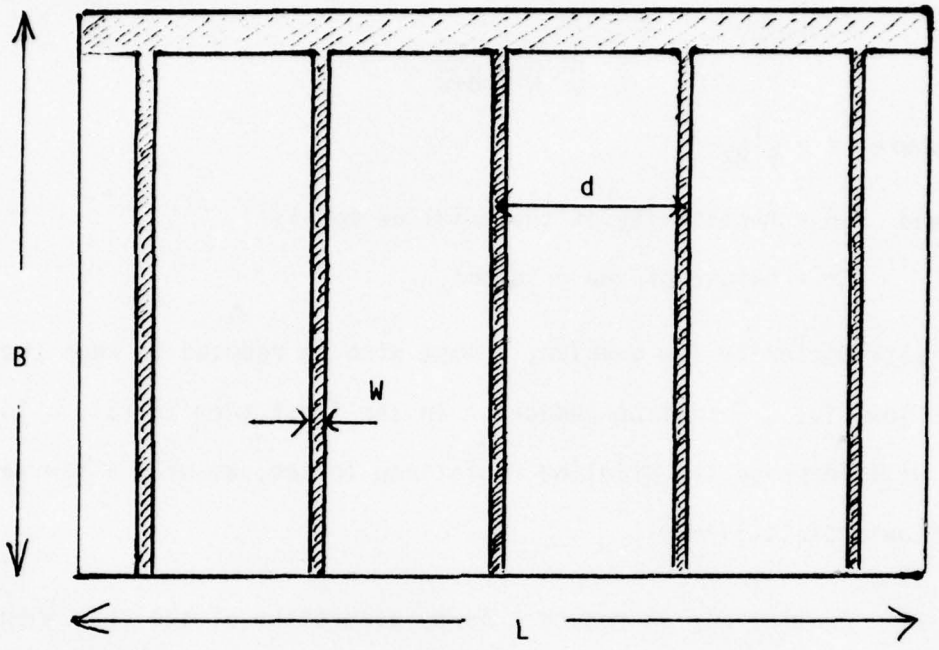

Explanation of Symbols

W = Gridline width

d = Grid to grid spacing

L,B = Length, width of cell

n = No. of grids = $\frac{L}{d}$

Figure 14: Cell and Grid Dimensions

We assumed d the grid spacing was chosen small enough to reduce the sheet resistance term to a low value, in practice requiring d < 0.15cm. The remaining two terms can be written as:

$$K \frac{\rho}{t} \frac{B}{L} \frac{d}{W} + \frac{W}{d+W} \qquad (2)$$

where $K = \frac{1}{1.8Z}$

and ρ = resistivity of the gridline metals.

t = height of the gridline.

For a satisfactorily low d-value, W must also be reduced to keep the shadow losses low, i.e., $\frac{W}{d}$ must be reduced. In the first term in (2), a low $\frac{W}{d}$ ratio will increase the gridline resistance losses, as will a low value of t (low profile lines).

2) *Another way to reduce* t is by alteration of the cell shape, in particular by increase of $\frac{L}{B}$, i.e., using a longer, narrower slice. At present, however, the contract goal of 2x2cm cells was retained and thus geometrical cell shape cannot be used to reduce grid height.

3) Another way to reduce grid height is to decrease ρ, the resistivity of the grid metals. Some attempts were made to design a means of applying a lateral electric field to the cell while depositing gridlines, but this was difficult and not pursued. An alternate method not fully explored either, involves replacing the electro-plated silver used mostly during this contract with evaporated silver, which could have reduced ρ. This would have meant developing a different method for applying the gridlines, and was not pursued, particularly since mid contract indications were that the deformation possibility had reduced the emphasis on low grid profile;

later in the contract it was realized that the higher profile increased the heating conditions required, with additional chance of degradation from contact interactions (see Section III-3c).

4) Another method to reduce the grid profile is to form grooves in the cell, and to locate the grids in these grooves. This approach was successfully demonstrated (some cells made this way were delivered with the final shipment) but it introduced several complications in cell processing. The groove patterns were readily made using photomasks similar to those used to form the grid contact pattern. However, it proved very difficult to realign the grid mask over the groove pattern. Small differences in the masks used led to some parts of the contact area not being fully placed in the grooves. Attempts to make extra large grooves led to a larger fraction of the area being non flat and therefore offset one of the main advantages of the cells made in the contract, namely over 90% flat area for bonding.

In addition slight variations in the alignment of the slice (particularly small rotations) gave lack of registration of all the fine gridlines. This difficulty in registration led to long times spent trying to register the grids in the grooves, and did not appear suited to a pilot production process. Some work was spent on modifications to the grooved contact approach, one where self-registration of the grids was attempted (this was difficult); another in which deeper diffused N+ regions were formed in the grooves, to provide dual resistance to degradation during ES bonding, namely both zero projection of lines above the surface, and reduced chance of adverse contact interaction with the shallow diffused layer

needed for the main PN junction. The grooved cells shipped in shipping lot #5 were of this type.

Note: As mentioned above, some of the impetus to develop all four low profile approaches further was removed by improvements in the ESB techniques.

b. Removal of Stray Metal

When stray metal was identified as a major problem in earlier ESB tests, several changes were made in cell processing. The stray metal arose mainly from photomask imperfections, which led to metal deposition in these "unwanted" areas . Often the stray metal deposits were not easily visible until after the electroplating step used to increase the gridline conductivity. Also the fixturing used in this plating step could lead to enhanced stray metal areas. Two main approaches were used, namely careful selection and handling of photomasks to minimize the leakage, sometimes suppliemented by the use of a coarser line mask closely spaced to the main mask, thus reducing leakage by the statistical reduction of the chance of coincident leakage areas on the two masks, and by protection of the fine line mask. Another method tested was the use of a coarser line shadow mask which blocked out much of the inter-grid area during evaporation of the contact metals.

Also some of the grooved contact schemes showed promise in reducing the stray metal. As was the case for the low profile tests, the later ESB technology with its deformation possibilities reduced the need to avoid this leakage, however, to ensure highest active area, and for schemes

where various protective layers were deposited under the gridlines it was advisable to minimize this leakage, and cells made later in the contract generally showed reduced leakage.

c. Increased High Temperature Contacts

With both the earlier and later ESB technology it appeared that ESB compatibility would be good if the cell contact structure could comfortably survive heating to ∿ 600°C for 5 to 15 minutes. Early ESB tests showed that an additional factor in cell degradation was the atmosphere (largely N_2) used in the ESB process while this HT was performed. Later ESB tests were performed in vacuo, or in an improved inert atmosphere; nevertheless, the typical cells shipped in shipping lot #4 degraded in ES bonding tests.

Two main approaches were tried to increase high temperature capability.

1) The use of various buffer layers under the grid contacts. Buffer layers tried were the phosphorosilicate glass remaining after diffusion, a thin layer of Ta_2O_5 or SiO, or a deeper N+ layer under the grids. The cells made with the dielectric layers had good high temperature capability, but it proved very difficult to find an adequate HT which could lead to the high CFF (> 0.77) needed to meet the contract goals. Also the use of the deep N+ layer involved an additional higher temperature diffusion step, and in some cases reduced the active area which had only the shallow N+ layer (the I_{sc} falls rapidly as the N+ layer depth is increased). Despite these difficulties, if future work is performed on improved high temperature contacts, these buffer layers are still worthy of consideration.

2) Use of different metal combinations. These tests mainly varied the metals used, to attempt to minimize degradation after HT. These high output cells generally require at least two metals, one to provide good adhesion and low contact resistance to the silicon, the other to provide high line conductivity. In addition, Pd is often added to provide improved moisture resistance. Although most of the metals used in these tests were of high purity, no systematic tests was made of the effect of varying purity on the degradation.

Choice of different bonding metals often combined attempts to provide a buffer layer to minimize solid state interdiffusion of the contact metals and silicon. For the grid contacts, the bonding metals most used were titanium, tantalum or chromium; in some cases tantalum was used in addition to the other two. Also palladium was sometimes included while the conducting metal used was mostly silver, although a few cells used gold in addition to silver. Thus front contact combinations tested included Ta-Ti-Pd-Ag, Ta-Cr-Au-Ag, Ti-Pd-Ag, Cr-Pd-Ag, Cr-Ag, Ti-Ag and Ta-Ag; these combinations were also evaluated in terms of their overall effectiveness at providing a fine line grid structure with good processing properties. Examination of the cells shipped shows that several of these combinations were submitted. The HT tests did not show that any clearly superior combination had been found. It must also be realised that with these metal layers, many cross-interactions are possible, and the literature abounds with descriptions of these phenomena. Also the deposition conditions can cause variations in behavior under HT, and clearly with the many combinations possible, many chances for variations exist.

The back contacts used were mainly Ti-Pd-Ag or Cr-Pd-Ag and at present the back contact is not considered the prime cause of cell degradation. However, in future work the effects occuring at both front and back surfaces of the cells must be separately identified.

Again as discussed above, the achievement of lower grid profiles proved to be beneficial to good ESB compatibility mainly because the HT cycle needed for good bonding was less severe. The suggestions for future work on ESB compatibility and the associate chance of increased hardness to laser irradation include additional work on studying various metal combinations and deposition methods, in addition to tests on lower profiles and buffer layers.

d. ES Bonding to the MLAR Layers

SPIRE's work has shown good bonding to AR coatings of SiO and Ta_2O_5 (formed in several different ways) but not to CeO_2. Therefore it is necessary to test new AR coating methods to ensure that a good ES bond is possible. Most of the MLAR coatings involved Al_2O_3 as the outer surface layer and early reports from both the Air Force and SPIRE indicated no problem in bonding 7070 glass to this layer. Some of the moisture resistance tests on the MLAR coatings (see Section V) involved additional outer coatings of SiO_2 or MgF_2; if such layers are used in future cells, or if different outer layers are used (such as ZrO_2) a preliminary test of ES bonding should be run to ensure that the bonding mechanism is still effective.

SECTION IV

CELLS SHIPPED

During the contract several shipments of cells ($\approx$ 100 cells) were made to demonstrate the various tests performed. At the end of the contract 100 cells were delivered. Details of the various shipments are given in the following tables; some notes on the shipments are also included.

1. First Shipment (See Table 5)

Twenty (20) 2x2cm cells were delivered to demonstrate the state-of-the-art. Twelve (12) of these cells had conventional diffusion and gridding, six (6) being coated with Ta_2O_5, the other six (6) with MLAR coating. The other eight (8) cells had violet cell diffusion and gridding; four (4) had Ta_2O_5 coating, the other four (4) had MLAR coating. The MLAR-coated cells were around 3% higher in short circuit current density than the corresponding Ta_2O_5-coated cells. However, this advantage would be decreased on covering, because the Ta_2O_5 cell increase by 2-3%, whereas the output of cells with MLAR coating shows only small changes on covering. The V_{oc} values were satisfactory. Overall the output of the best cells was about 7.5% below the contract goal. About one-third of the deficit (2-5%) could be traced to low CFF, possibly from inadequate grid formation. The remaining losses ($\sim$ 5%) were mainly in I_{sc}, and of this perhaps 2.5% resulted from less active area than optimum, and the remaining 2.5% was lost in the MLAR coating.

TABLE 5

FIRST CELL SHIPMENT

TEST CONDITIONS: AMO, set with BF violet cell #104, cells at 24°C, cells 2x2cm

Cell No.	Voc (mV)	Isc (mA)	P_{500} (mW)	CFF	Comments
988 - 1	598	144.3	67.6	.78	Conventional Diffusion
2	595	143.9	63.1	.73	Ta_2O_5 AR
3	597	145.5	62.3	.71	
4	605	146.1	67.3	.76	
5	600	140.5	66.7	.79	
6	600	143.2	67.9	.79	
7	602	149.1	70.4	.78	Conventional Diffusion
8	602	149.8	70.8	.78	MLAR
9	600	148.8	70.6	.78	
10	598	147.2	69.6	.79	
11	599	144.1	68.5	.79	
12	599	145.0	66.9	.77	
13	601	150.4	71.4	.78	Violet Cell Ta_2O_5 AR
14	601	150.0	71.6	.79	
15	597	148.6	68.4	.77	
16	603	148.5	68.3	.76	
17	604	156.8	73.9	.78	Violet Cell MLAR
18	605	156.2	72.8	.77	
19	604	156.8	73.2	.77	
20	603	156.0	72.3	.77	

2. Second Shipment (See Table 6)

Around twenty (20) cells were shipped. They included a few control cells with Ta_2O_5 coating, some conventional cells with MLAR coating, and the rest were violet cells with MLAR coating variations.

There were four different coating combinations (high index Ta_2O_5, medium index Ta_2O_5 plus Al_2O_3, high index Ta_2O_5 plus Al_2O_3, and high index TiO_x plus Al_2O_3. The best power output achieved was $\sim$ 74mW, and with the cover gain measured, this should increase to $\sim$ 76mW.

These shipped samples were not visually good, because of some contact deficiencies, and also because the cell processing used gave partial attack of some of the MLAR coatings.

3. Third Shipment (See Tables 7 and 8)

Twenty-six (26) cells were shipped. Three different coatings were used (TiO_x-Al_2O_3, Ta_2O_5-Al_2O_3, and for control Ta_2O_5). Also three different front contact metal combinations were used, with two different back contact stacks.

This group included mostly cells with 10 gridlines per centimeter, but cells with 20 and 40 lines per centimeter were included to show the tradeoffs involved in the low profile tests.

Table 8 gives the electrical results obtained on the cells. Several combinations of I_{sc}, V_{oc} and CFF can be seen; for example, the highest I_{sc} values are often associated with slightly reduced CFF values. Several of these cells approached the contract goal of 81mW (15%).

TABLE 6

SECOND CELL SHIPMENT

TEST CONDITIONS: AMO, set with BF violet cell #104, cells at 25°C, cells 2x2cm.

Cell No.	Front Contact Configuration	AR Layer* #1	AR Layer #2	Voc (mV)	Isc (mA)	CFF	Pm (mW)	Cover Gain (%)
988 - 21	20 Lines	Ta_2O_5 (H)	---	601	144.1	.78	68.4	---
22	+ Bar Contact	"	---	600	151.5	.78	70.8	3.4
23		"	---	597	146.2	$.77_5$	67.7	---
24		"	---	601	149.8	.78	70.5	4.8
25	8 Wide Lines	Ta_2O_5 (M)	Al_2O_3	596	148.9	$.73_5$	65.3	---
26	+ Wide Bar	"	"	599	148.6	$.76_5$	68.2	1.0
27		"	"	598	147.0	$.77_5$	68.3	0.6
28		"	"	592	146.1	.79	68.2	---
29	20 Lines	Ta_2O_5 (H)	Al_2O_3	602	154.9	$.78_5$	73.4	1.9
30	+ Bar Contact	"	"	606	156.1	$.78_5$	74.3	1.5
31		"	"	606	152.8	.79	73.2	2.0
32		"	"	604	156.8	.77	73.1	---
33		"	"	606	154.4	$.78_5$	73.7	1.7
34		"	"	604	152.7	.78	72.3	---
35		"	"	603	155.3	.78	73.4	1.9
36		"	"	608	151.7	$.77_5$	71.7	1.8
37		"	"	602	152.8	.78	71.8	---
38	20 Lines	TiOx (H)	Al_2O_3	604	162.3	$.72_5$	71.1	1.7
39	+ Pads	"	"	603	160.9	$.76_5$	74.2	2.2
40	20 Lines	TiOx (H)	Al_2O_3	600	150.7	.79	71.6	3.1
41	+ Bar Contact	"	"	602	147.6	$.78_5$	70.0	2.9

*H, M refer to high, medium refractive index.

TABLE 7

THIRD SHIPPING LOT

CELL DETAILS

Cell #	AR Coating	Contact Metals		Grid/cm
		Front	Back	
988 - 42	T_iO_x - Al_2O_3	a	c	10
43	"	a	c	10
44	"	a	c	10
45	"	a	c	10
46	"	a	c	10
47	"	a	c	10
48	"	a	c	10
49	"	a	c	10
50	"	a	c	10
51	"	a	c	10
52	"	a	c	10
53	"	a	c	10
54	"	b	Pd-Ag	10
55	"	a	c	10
56	"	b	c	10
57	Ta_2O_5 - Al_2O_3	d	d	10
58	"	d	d	10
59	Ta_2O_5	d	d	10
60	Ta_2O_5 - Al_2O_3	d	d	10
61	Ta_2O_5	d	d	10
62	Ta_2O_5 - Al_2O_3	d	d	10
63	Ta_2O_5 - Al_2O_3	d	d	10
64	Ta_2O_5	d	d	10
65	Ta_2O_5 - Al_2O_3	d	d	20
66	Ta_2O_5	d	d	40
67	Ta_2O_5 - Al_2O_3	d	d	40

Notes: (a) - Ta-Cr-Au-Ag
(b) - Ta-Ti-Pd-Ag
(c) - Cr-Pd-Ag
(d) - Cr-Au-Ag

TABLE 8

THIRD SHIPPING LOT

I-V MEASUREMENTS

TEST CONDITIONS: AMO, set with BF violet cell #104, cells at 25°C, cells 2x2cm

#	Voc (mV)	Isc (mA)	Tu (mA)	Xe (mA)	I_{500}	P_{500}	Pm (mW)	CFF
42	600	164	96	67	148	74	73.6	.76
43	605	166	93	72	153.5	76.7	76.5	.76
44	605	163	95	68	149	74.5	74.2	$.75_3$
45	602	160	92	69	152.5	76.2	76.5	.80
46	602	164	95	71	149	74.5	74.4	.75
47	605	160	91	69	151.5	75.7	74.4	$.75_6$
48	610	160	92	69	154	77	78	.80
49	615	165	94	72	158	79	78.8	$.77_6$
50	610	164	93	69	154	77	77.8	$.78_7$
51	610	166	96	71	156	78	77.8	.77
52	610	160	92	69	151	75.5	75.2	.77
53	605	167	95	72	152	76	76.2	$.75_5$
54	605	161	94	69	152	76	76.7	$.78_8$
55	607	161	92	70	152	76	75.2	.77
56	610	165	95	71	158	79	79.8	.79
57	610	160	98	63	155	77.5	78.5	$.80_4$
58	610	158	96	63	151	75.5	75.7	$.78_5$
59	605	153	88	65	143.5	71.7	72.4	.78
60	605	164	100	66	153	76.5	76.8	$.76_9$
61	602	155	88	68	142	71	70.8	$.75_9$
62	610	160	96	65	138	69	71.2	.73
63	610	163	99	63	148	74	73.8	$.74_2$
64	607	154	90	64	140	70	69.8	$.74_6$
65	600	155	93	62	146	73	73.4	.79
66	600	147.5	84	64	136	68	67.9	$.76_7$
67	600	148.5	90	69	140	70	70	$.78_6$

4. Fourth Shipment (See Table 9)

Twenty-seven (27) cells were delivered, twelve (12) to SPIRE for ESB tests, the other fifteen (15) to the Air Force. Because some cells were slightly oversize, Pm values corrected to $4cm^2$ have been included.

All the cells had TiO_x-Al_2O_3 AR coatings.

5. Fifth Shipment - Final Shipment (See Tables 10 and 11)

This shipment included:

100 - $2x2cm^2$ cells

4 - $2x4cm^2$ to show the output for the large cells

4 - Grooved cells

A curve showing the Pmax distribution of the 100 cells is given in Figure 15.

The average coating gain was 1.45 ± .01; with the measured cover gain, the overall covered ratio was 1.47 ± .01.

6. Yield for Shipping Lots #4 and #5

These lots comprised 135 cells. They were selected as follows:

The starting slices were processed to give uncoated cells and I-V measurements were used to screen out all cells with output below 50mW. Those with output above 50mW were visually checked and then coated with MLAR layers. The cells were then remeasured and cells > 74mW and with good visual appearance were shipped.

TABLE 9

FOURTH SHIPPING LOT

CELL DETAILS

TEST CONDITIONS: AMO, measured with BF violet cell #104, cell temperature 25°C, cells 2x2cm

Cell No.	Voc (mV)	Isc (mA)	Pm (mW)	Pm* (mW)	Cover Gain (%)
988 - 68	610	164.5	77.9	76.5	+2
69	612	158.9	77.1	76.6	+0.6
70	610	162.5	78	76	+2.6
71	608	160.1	76.2	74	
72	610	159.5	75.6	73.8	
73	610	162.3	77.3	75.7	
74	609	158.6	76.2	74.9	
75	609	160.2	77.7	76.4	
76	610	163.4	77.6	75.6	
77	611	158.3	75.8	75	
78	609	154.6	74.8	72.8	
79	611	159.9	74.8	74.4	
80	611	158.9	76.1	75.8	0.6
81	610	160.2	76.5	74.3	
82	605	161.0	76.4	74.4	
83	607	161.4	75.7	73.3	
84	610	159.1	75.4	73.4	
85	605	161	74.6	75.9	
86	612	161.3	77.8	75.7	0.5
87	610	162.4	75.7	75.6	
88	611	158.0	76.3	74.2	
89	609	165.4	78.0	75.9	
90	610	162.0	78.7	76.6	
91	613	164.1	76.7	75.1	
92	607	158.3	76.4	74.8	
93	604	159.1	75	72.9	
94	608	161.7	77.3	74.8	

*Corrected to $4cm^2$

The approximate yield can be seen by the following numbers:

No. of starting slices	$\approx$ 650 (100%)
Visual Rejects	$\approx$ 75 (11.5%)
Electrical Rejects	$\approx$ 440 (67.5%)
Good Cells	$\approx$ 135 (21%)

The highest losses are from the electrical yield of the uncoated cells. The MLAR coating process itself had high yield.

Some individual lots were better, giving an overall shippable yield from starting slices of 42%, which corresponded to over 50% electrical yield in these lots.

TABLE 10

FINAL SHIPMENT

(100 CELLS)

TEST CONDITIONS: AMO, measured with BF violet cell #104, cells at 25°C, cells 2x2cm

Cell No.	Voc (mV)	Isc (mA)	Pm (mW)	Pm* (mW)	Pm$^{\emptyset}$ (mW)
988 - 95	609	163	78	76.3	77.4
96	608	155.6	76	75.5	76.7
97	608	156.9	75.5	74.5	75.6
98	610	155	76.2	75.3	76.4
99	606	158.1	76.5	76.2	77.3
100	604	161.7	77.3	75.3	76.4
101	604	160.3	75.8	75.8	76.9
102	607	160	76.5	74.2	75.3
103	608	156.8	76	74.8	75.9
104	611	158.7	76.8	75.9	77
105	610	165.0	78.7	76.7	77.9
106	609	160.2	78.1	77.2	78.3
107	607	155.9	75.6	74.8	75.9
108	606	158.7	76.9	74.4	75.5
109	602	159	76.1	75.3	76.5
110	608	157.3	75.1	74.3	75.5
111	609	160.4	76.1	73.7	74.8
112	610	153.9	74.8	74	75.1
113	604	159.2	76	76.8	77.9
114	601	160	76.1	75.5	76.6
115	606	161	77.1	74.8	75.9
116	607	155.8	75.1	74.6	75.7
117	605	155.7	75.2	74.8	75.9
118	603	161.2	75.8	75.7	76.9
119	604	163.5	77.2	75.5	76.6

* Corrected to $4cm^2$ area.

$\emptyset$ Further corrected for 1.5% cover gain.

TABLE 10 (Continued)

FINAL SHIPMENT

(100 CELLS)

TEST CONDITIONS: AMO, measured with BF violet cell #104, cells at 25°C, cells 2x2cm

Cell No.	Voc (mV)	Isc (mA)	Pm (mW)	Pm* (mW)	Pm^{Ø} (mW)
988 - 120	609	155.3	75.7	74.9	76
121	605	155.9	75.5	73.1	74.2
122	601	159	76.1	73.7	74.2
123	603	157.5	76	75.3	76.4
124	602	162.2	76.7	74.9	76
125	609	160	76.6	76.3	77.4
126	606	161	75.5	74.6	75.7
127	603	161.5	75.7	73.3	74.4
128	606	161.2	75	72.5	73.6
129	604	163.1	74.5	----	----
130	607	163.5	74.8	72.2	73.3
131	612	158.5	75	75	76.1
132	609	163.7	76.5	74.9	76
133	609	158.8	74.6	75.3	76.5
134	605	164.5	77.8	77.3	78.5
135	606	168.8	80.8	78.6	79.8
136	607	158	74.6	74.2	75.3
137	607	156.6	74.2	74.2	75.3
138	606	156.6	74.6	74.5	75.6
139	605	158.5	75.2	74	75.1
140	610	163.7	76.5	75.5	76.6
141	609	159.7	75.5	76.5	77.6
142	607	161.4	78	76.1	77.2
143	603	162.5	75.7	74.6	75.8
144	603	159.9	76	75.6	77.9

* Corrected to $4cm^2$ area.
Ø Further corrected for 1.5% cover gain.

TABLE 10 (Continued)

FINAL SHIPMENT

(100 CELLS)

TEST CONDITIONS: AMO, measured with BF violet cell #104, cells at 25°C, cells 2x2cm

Cell No.	Voc (mV)	Isc (mA)	Pm (mW)	Pm* (mW)	Pm$^{\emptyset}$ (mW)
988 - 145	600	163.5	75	72.8	73.9
146	606	167.7	75.5	72.8	73.9
147	608	162.9	74.2	72	73.1
148	612	159.3	77.5	77.1	78.2
149	609	160.7	75.8	73.7	74.8
150	604	162.3	74.5	73	74.1
151	601	162.5	74.5	72.8	73.9
152	609	163	78.2	76.1	77.2
153	608	160.4	75.1	74.3	75.4
154	608	161.5	74.1	73.1	74.2
155	608	161.5	76.6	75.5	76.6
156	607	158.4	74.5	74	75.1
157	608	158.6	74.8	74.7	75.8
158	604	162.5	75	73.9	75
159	605	158.6	74.5	74.1	75.2
160	606	156.8	74.6	74.6	75.7
161	608	159.1	74.8	72.4	73.5
162	603	162	74.8	72.9	74
163	604	165.1	77.9	77.1	78.2
164	608	168.7	79.7	78.4	79.6
165	607	166.8	79.1	77	78.2
166	605	159.1	74.8	74	75.1
167	606	165.5	77	76.9	78
168	608	162	77.4	76.9	78.1
169	610	165	79.4	77.3	78.4

* Corrected to $4cm^2$ area.

$\emptyset$ Further corrected for 1.5% cover gain.

TABLE 10 (Continued)

FINAL SHIPMENT

(100 CELLS)

TEST CONDITIONS: AMO, measured with BF violet cell #104, cells at 25°C, cells 2x2cm

Cell No.	Voc (mV)	Isc (mA)	Pm (mW)	Pm* (mW)	Pm$^{\emptyset}$ (mW)
988 - 170	606	157.3	75.5	75	76.1
171	605	161.1	75.4	73.1	74.2
172	610	157.6	75.5	73.8	74.9
173	602	158.1	74.2	74.9	76
174	602	160.7	74.7	73.5	74.6
175	607	158.6	75.2	74.1	75.2
176	608	162.8	75.1	73.7	74.8
177	602	158.6	74.9	74.4	75.5
178	607	159.2	76	74.8	75.9
179	606	157.4	74	73.7	74.8
180	608	159.4	74.5	72.3	73.4
181	610	156.5	74.5	72.3	73.4
182	613	164	77.6	75.2	76.3
183	606	160	75.7	75.3	76.4
184	607	159.8	76.5	74.4	75.5
185	611	162	76.1	74.1	75.1
186	613	164.1	77.8	75.6	76.7
187	606	159	76.9	74.8	75.9
188	609	156.7	75	75.8	76.9
189	607	158.7	77.3	75.1	76.3
190	605	160	74.8	73.6	74.7
191	610	163.4	79.4	77.6	78.9
192	607	160	77.3	77.1	78.3
193	609	154.9	75.2	74.8	75.9
194	607	163.9	78.6	----	----

* Corrected to 4cm^2 area.

$\emptyset$ Further corrected for 1.5% cover gain.

TABLE 11

FINAL SHIPPING LOT

TEST CONDITIONS: AMO, measured with BF violet cell #104, cell temperature 25°C

#	Voc	Isc	Pm*	Size (cm)	Comments
988 - 196	607	314.7	151.6	2 x 4	To Illustrate Larger Area Performance
197	602	322.1	152.8		
198	609	327.4	153.6		
199	604	315.1	152.0		
988 - 200	585	220.8	100.8	2 x 4 No AR	
201	579	216.9	97.3		
202	593	150.5	68.2	2 x 2 + AR	Grooved Contact Cells
203	595	160.3	69.5		

* Not corrected for exact area.

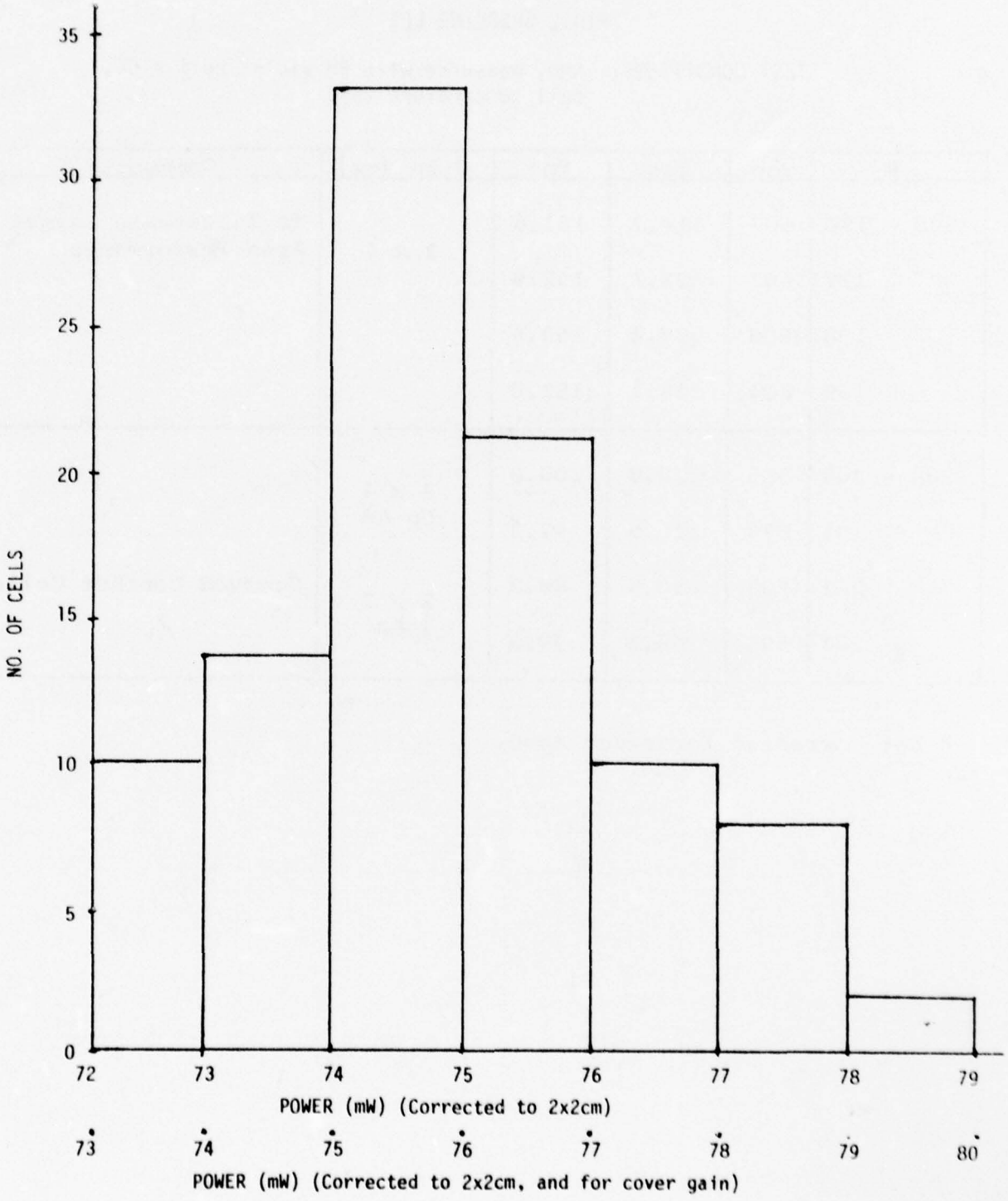

Figure 15: Power Output for Final Shipment

SECTION V

ENVIRONMENTAL TESTS

1. Contact Adhesion Tests

The contact adhesion was tested using a parallel gap welding test. Most of the contact systems tested were weldable. For front surface contacts, the average pull strength at which contact failure occurred at 90° pull angle was around 120gm. For back contacts as used here the average pull strength was 90gm. For chemically polished backs, the average pull strength was 350gm. Even at the lowest pull strengths, silicon was removed in craters. This may be adequate from the viewpoint of technically passing a contact pull test, but indicates the high stresses which can exist in these metal sandwiches. The pull strength was increased fivefold when pulled at 0° to the cell surface.

2. Heat Treatment Tests

In addition to the tests described in Section III-3f some of the cells similar to those shipped towards the end of the contract were given various heat treatments. The results are shown in Table 12.

V_{oc} - The HT in N_2 showed severe loss in V_{oc}. In all but one case, HT in H_2 even at 600°C did not degrade V_{oc}.

I_{sc} - In all cases, I_{sc} was not affected greatly by the HT.

I_{500} - The best results were 500°C - 10 minutes in H_2, suggesting that the 500°C - 5 minutes HT was not sufficient to reduce the contact resistance fully. The HT at 600°C in H_2 showed loss of I_{500} partly

TABLE 12

HEAT TREATMENT TESTS ON CELLS

HT Conditions	Before or After	Isc	Voc	I_{200}	I_{500}
500°C-5 Min.-H_2	B	158	605	158	166
	A	160	595	160	139
	B	157	600	156	128
	A	162	600	162	147
500°C-10 Min.-H_2	B	156.5	600	157	142
	A	158	590	156	142
	B	156	600	156	147
	A	156	600	156	147
600°C-5 Min.-H_2	B	156	600	156	138
	A	158	600	156	128
	B	156	600	156	143
	A	158	500	146	---
600°C-10 Min.-H_2	B	156	600	155	142
	A	156	340	116	---
	B	158	600	157	145
	A	157	590	152	104
600°C-5 Min.-N_2	B	158	605	158	149
	A	158	535	149	30
	B	157	600	156	143
	A	158	540	149	35
600°C-10 Min.-N_2	B	156	600	156	145
	A	156	385	125	---
	B	157	595	156	135
	A	156	525	137	20

because V_{oc} was decreased, but some additional losses in CFF are seen. The I_{500} losses in N_2 were a combination of decreased V_{oc} and CFF.

Comment - These tests indicate the sensitivity of the cell output to both the HT temperature-time schedule, but equally important also to the atmosphere in which the HT is performed. This conclusion has implications in the ESB compatibility tests, showing the importance of the atmosphere present while the cells are being bonded.

3. Temperature Cycling Tests

Cells subjected to twenty (20) cycles (liquid N_2 to boiling water) showed little or no degradation.

4. Humidity Tests

Ten (10) cells were run at 65°C, > 95% relative humidity for 30 days. The electrical results before and after the test are shown in Table 13.

V_{oc} - There was no significant change in V_{oc} observed except for cell #70.

I_{sc} - Only cell #70 showed any loss in I_{sc}.

I_{500} - The increase in I_{500} for cell #2 probably indicated inadequate contact during testing before the humidity test. Seven (7) other cells changed by $\sim$ 1%. Cell #87 decreased by $\sim$ 5.5%, and #70 as expected from the V_{oc} loss had lost almost all output.

These results indicate adequate humidity resistance.

TABLE 13

HUMIDITY TEST I-V READINGS

Cell #	Before/After	Voc	Isc	I_{500}	I_{520}
2	B	608	160.6	147.9	138.7
	A	608	159.4	152.6	147.1
18	B	602	159.7	147.8	138.1
	A	602	157.9	145	133.7
30	B	605	157.7	148.1	142.3
	A	606	156.5	147.1	141.4
55	B	606	156.3	146.4	139.3
	A	607	155.3	147.5	141.3
57	B	603	161.6	149.2	140.8
	A	602	159.8	148.7	141.5
61	B	609	163.8	153.5	145.9
	A	608	162.6	151.9	144
66	B	606	155.5	147.3	140.8
	A	606	154	146.2	140.3
70	B	605	158.7	146.1	140.7
	A	40	138.5	-----	-----
87	B	603	157.1	146.9	139.5
	A	605	156.7	138.9	127
94	B	609	157	146.3	139.2
	A	609	156.2	147.2	140.8

5. Moisture Tests

MLAR cells shipped early in the contract had visual deficiencies, caused by etch leakage (HNO_3 and/or HF) while edge etching the cells. The attack was confined to a picture frame around 2mm wide, and involved removal of the Al_2O_3 outer layer. The effect on reflectance of this gradual removal of Al_2O_3 in the MLAR is shown in Figure 16.

Later some cells showed visual changes during moisture exposure (immersed in boiling water for 10-30 minutes, or suspended in wet steam for 10-30 minutes). Those changes were attributed to partial or near complete removal of Al_2O_3, but it was only observed on $\sim$ 10-20% of the cells tested. This suggested that this moisture susceptibility depended on the deposition conditions or the post coating heating.

In tests of MLAR coatings using more than two layers, additional layers were added to the DLAR.

$\underline{MgF_2}$

A fairly thin layer of MgF_2 was tried. The I-V values for the MLAR cell were not changed much by the additional MgF_2 layer (perhaps increase $\sim$ 1%). The effect of the additional layer on reflectance is shown in Figure 17.

$\underline{SiO_2}$

Also a series of various thicknesses of SiO_2 was tested. The SiO_2 coatings appeared to improve the moisture resistance. Layers $\sim$ 2200, 4400, 6600, 8800, 11000Å thick were added. The effects on the I-V parameters

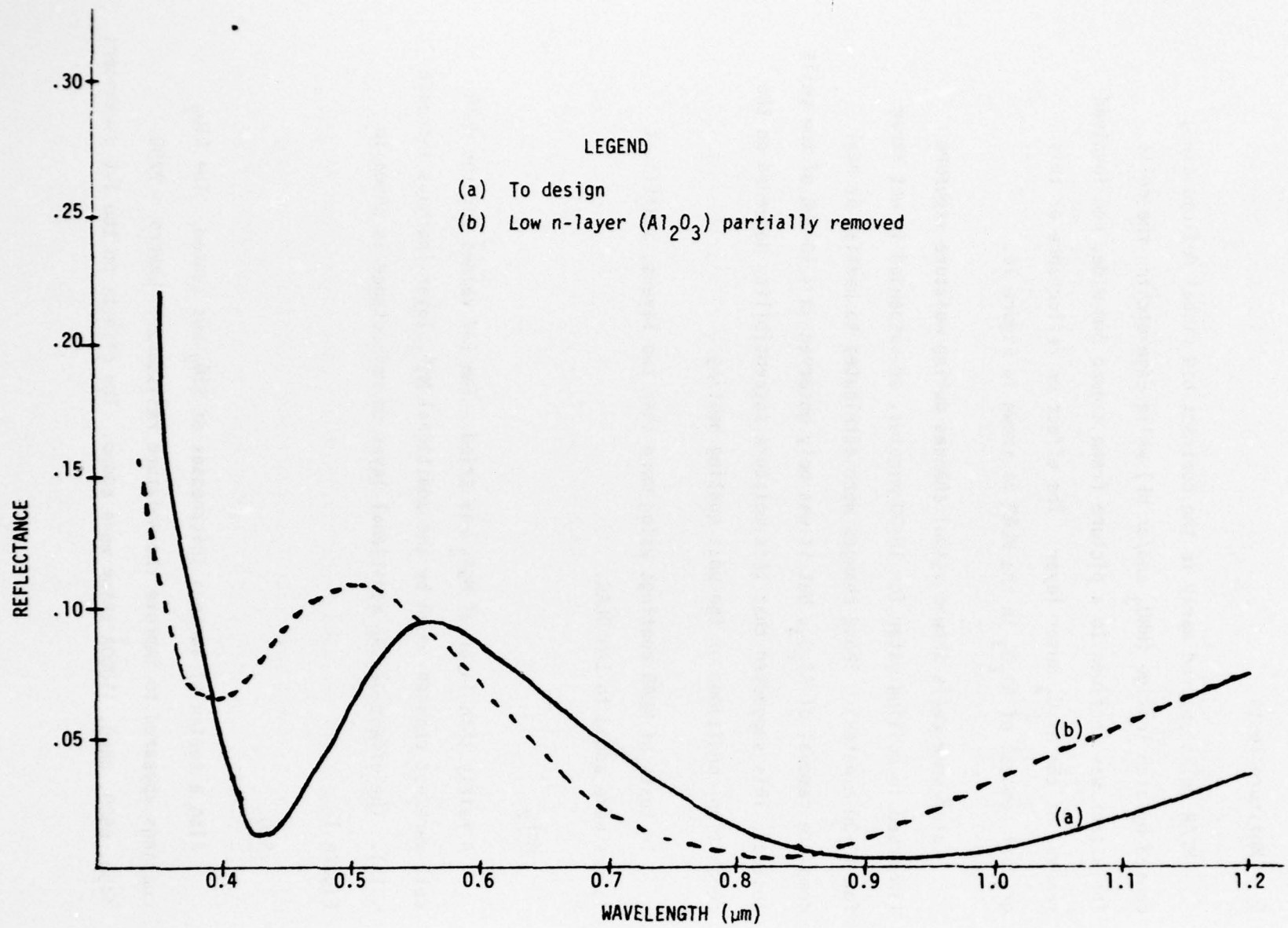

Figure 16: Reflectance - Wavelength for DLAR Coating on Cell

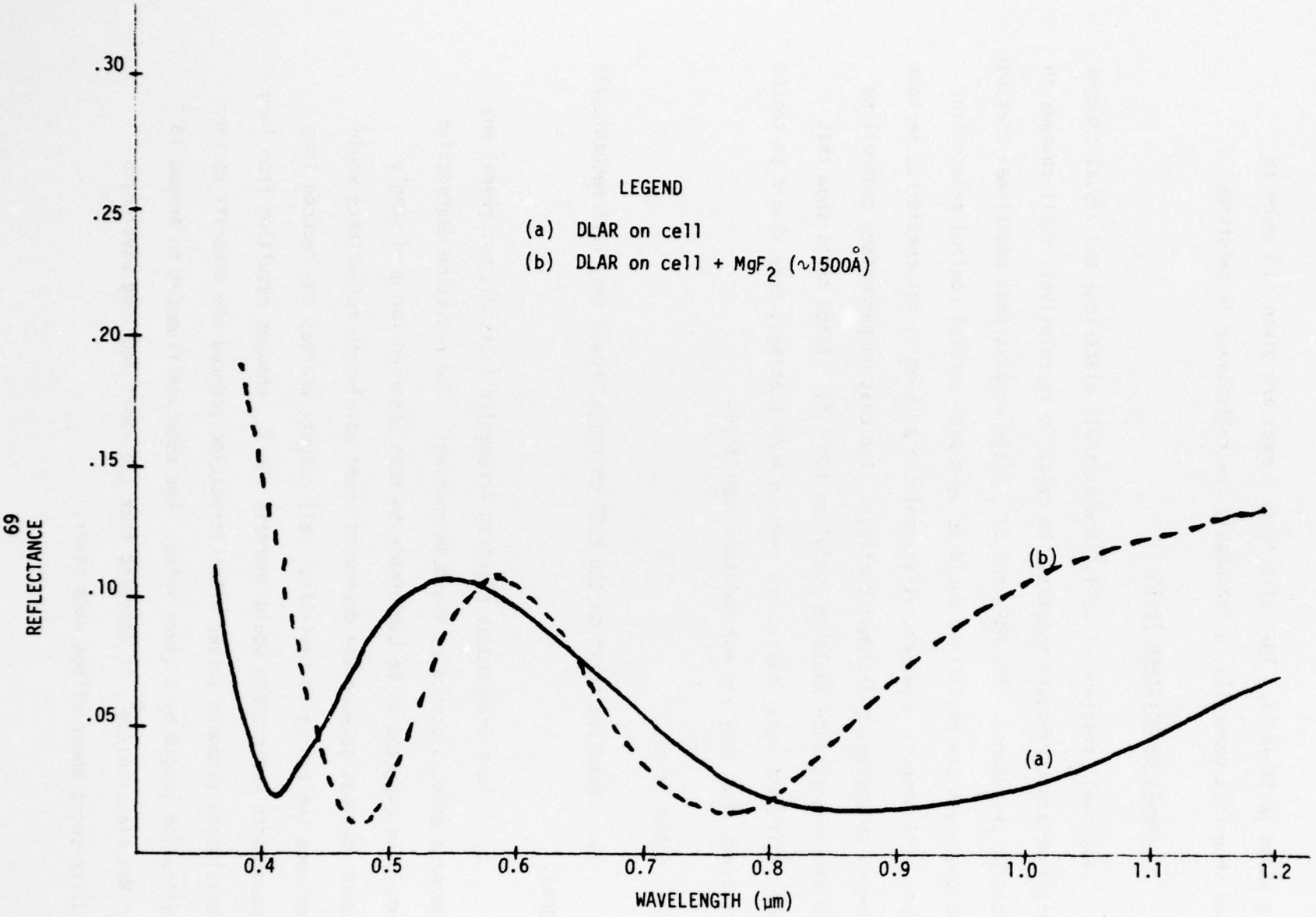

Figure 17: Reflectance - Wavelength for DLAR on Cell + M_gF_2

is shown in Table 14. The reflectance curves are given in Figure 18 and show that generally, a reasonably low reflectance is maintained.

Comments on Moisture Tests

The small fraction of cells showing small electrical and visual changes after moisture exposure suggests the cause is in relatively small changes in coating procedures. The MgF_2 and SiO_2 tests suggest that additional coatings of good moisture resistance could be used with careful control maintaining good cell output. However, at present the problem is not considered serious enough to warrant additional coatings. The coating parameters controlling moisture resistance would be useful to identify. These tests show that when different outer layers are used in MLAR coatings, they should be tested to check that they are not moisture sensitive.

6. Other Tests

1) Handling tests on the MLAR coatings showed they were mechanically good.

2) Some independent electron irradation tests did not reveal any adverse effects caused by the MLAR coatings. The radiation degradation would be expected to be comparable to that observed for good single QWAR coatings because the decreased short wavelength reflectance would enhance the radiation resistanct cell output, whereas the reduced long wavelength reflectance would increase the I_{sc} changes resulting from long wavelength response losses after irradation reduced the minority carrier diffusion length by a given value. For electron fluences to around 10^{15} 1 Mev electrons/cm^2, it appeared that the short and long wavelength differences about offset each other.

TABLE 14

PERCENTAGE CHANGES IN I-V PROPERTIES FOR
MLAR COATED CELLS PLUS VARIOUS SiO_2 THICKNESSES

Cell	AR	Δ Isc	Δ Long λ	Δ Short λ	Δ I_{500}
1	MLAR + 2200Å SiO_2	-3	-4	-1.4	-1.8
2	MLAR + 4400Å SiO_2	-0.8	0	-1.4	+3
3	MLAR + 6600Å SiO_2	-2.3	-2	-2.1	-1.5
4	MLAR + 8800Å SiO_2	-1.2	-0.5	-2.1	+0.8
5	MLAR + 11000Å SiO_2	-2.2	-2	-1.7	+1.4
6	MLAR + 13200Å SiO_2	-3	-2.3	-3.6	-2.5

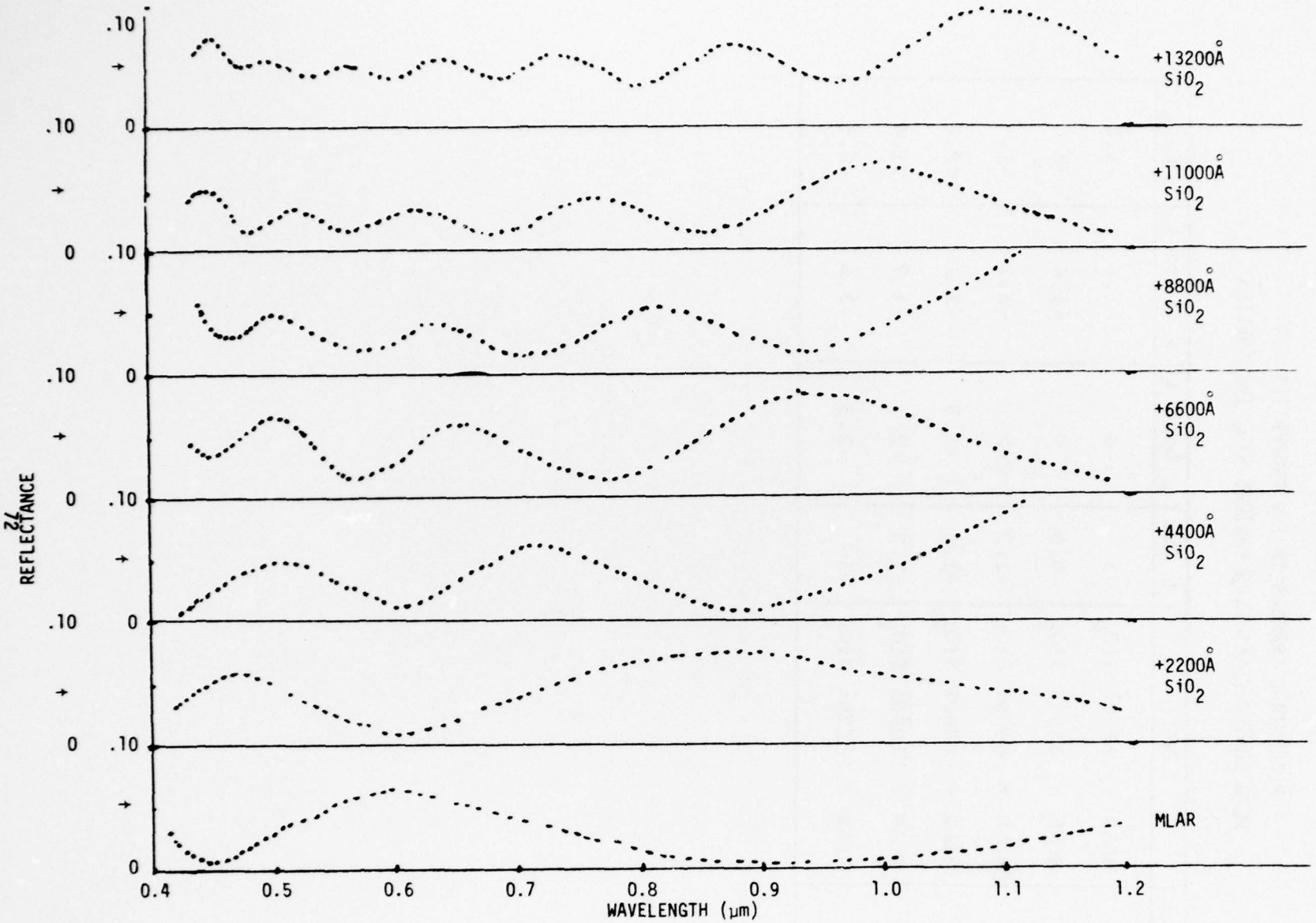

Figure 18: Reflectance of MLAR on Cells + Various SiO_2 Thicknesses

SECTION VI

COMMENTS AND CONCLUSIONS

1. Comments

The contract resulted in uncoated cells of high efficiency, obtained by combining present-day methods, namely using good quality silicon, a shallow PN junction of good quality, and a grid pattern consisting of many ($\sim$ 10 per cm) narrow gridlines of good conductivity. These cells could be coated by MLAR coatings which increased the bare cell output by factors up to 1.46 to 1.48. When covered these cells could have overall gain factors 1.46 to 1.50. In absolute terms, the power output under AMO illumination of $4cm^2$ cells at 25°C could lie in the range 74-80mW. The various factors controlling cell output before and after coating were described above, and the key factors were identified. It was shown that these cells could be processed in a production like facility. The surface finish of the completed cells was suited to electrostatic bonding, and there appeared to be no difficulty in bonding to MLAR coatings with Al_2O_3 as the outer dielectric layer.

Despite tests using several different contact metal combinations, these cells did not appear capable (with good yield) of withstanding the combined temperature-pressure-time sequence involved in current ES bonding. The failure was apparently interaction of some of the metals used with the PN junction. As described in Section III-3 tests were made to improve the ESB compatibility, by reducing the grid profile, or trying alternate metals. However, none of the methods tried showed promise of meeting the high output requirements of the cells or of maintaining a reasonably uncomplicated process sequence.

The cells made in this contract appear satisfactory in most of the environmental tests described in Section V (and for in-line process capability), but as explained, there were signs of some moisture degradation on some of the AR coating materials, especially those with moderate refractive indices.

2. Conclusions

This contract met the contract goals in power output from MLAR coated cells, with fair yields (see Section IV-6). The cell processing including the MLAR coating step were all capably performed in a production-type fashion.

There is more work needed to extend the cell capability to the full ESB processing. At present it is considered that this can be achieved by selection and control of suitable contact systems. Promising system are those combining a refractory metal as the barrier layer, and silver as conducting layer. If additional metals are included it would be mainly to ensure good performance in moisture exposure.

SECTION VII

RECOMMENDATIONS

This work was initiated to identify the highest power output non-textured finish cells which could be satisfactorily combined with ES bonded covers. The conclusions above show that there is still need for more work to develop suitable contact systems which can maintain high cell output before and after ES bonding. In addition, such contacts are probably those with promise in providing resistance to degradation by high intensity laser irradiation.

There are also additional AF tests planned to apply ES bonding to textured surface cells. The contact systems applicable to polished cells should also have corresponding advantages for the textured surfaces, and this is an additional reason for suggesting future work on suitable contact systems.

REFERENCES

1. J. Lindmayer, J. Allison, "The Violet Cell," Proceedings 9th IEEE Photovoltaic Specialists Conference (1972), p. 83.

2. J. Haynos et.al., "The COMSAT Non-Reflective Cell," Proceedings of the International Conference on Photovoltaic Power Generation (1974) p. 487.

3. J. P. Schwartz, "Improved Silicon Solar Cell Antireflective Coatings," Proceedings of 8th IEEE Photovoltaic Specialists Conference, (1970) p. 173.

4. G. Seibert, "Increased Solar Cell Output By Improved Optical Matching," Part 1, Theoretical-ESR TN-90 (ESTEC) Part 2, Experimental-ESRO TN-91 (ESTEC) (1969).

5. "Low Reflectivity Solar Cells," (Spectrolab) AFAPL- TR-75-98.

6. J. Apfel, "Antireflection Coatings for Semiconductors," Proceedings of Symposium on the Material Science Aspects of Thin Film Systems for Solar Energy Conversion, (1974) p. 276.

7. A. Kirkpatrick, "Integrally Bonded Covers for Silicon Solar Cells," Proceedings of 11th IEEE Photovoltaic Specialists Conference, (1975) p. 169.